Effective Speed Tracking Control of Permanent Magnet Synchronous Motor using Disturbance Observer aided Sliding Mode Control

by

Miras Akhmetov

Submitted to the Department of Robotics and Mechatronics
in partial fulfillment of the requirements for the degree of

Master of Science in Robotics

at the

NAZARBAYEV UNIVERSITY

Apr 2025

Author .....
Department of Robotics and Mechatronics
Apr 29, 2025

Certified by .....
Ton Duc Do
Associate Professor
Thesis Supervisor

Accepted by .....
Yelyzaveta Arkhangelsky
Dean, School of Engineering and Digital Sciences

Effective Speed Tracking Control of Permanent Magnet Synchronous Motor using Disturbance Observer aided Sliding Mode Control

by

Miras Akhmetov

Submitted to the Department of Robotics and Mechatronics
on Apr 29, 2025, in partial fulfillment of the
requirements for the degree of
Master of Science in Robotics

Abstract

This thesis presents the design and implementation of a robust speed tracking control strategy for Permanent Magnet Synchronous Motors (PMSMs) by integrating Sliding Mode Control (SMC) with a Disturbance Observer (DOB). PMSMs are widely used in industrial and high-performance applications because of their efficiency, compact size, and dynamic performance. However, they are vulnerable to external disturbances and nonlinear dynamics, which makes it harder to achieve a precise control

To address these problems, an SMC is developed to ensure robustness against parametric uncertainties and external disturbances. The analysis includes both matched and mismatched disturbance cases. To improve the disturbance rejection, a DOB is added to estimate and compensate for external torques, frictional effects, and model inaccuracies in real-time. A comprehensive analysis of the system's frequency-domain characteristics is conducted, showing how DOB parameters influence sensitivity and robustness.

Simulation and experiments are carried out on a 300W PMSM. Comparative results between conventional PI control and the proposed SMC-DOB structure under different loads and inertia conditions reveal that the DOB-aided SMC provides superior tracking accuracy, faster transient response, and improved disturbance rejection. These results confirm the effectiveness of the proposed strategy for precise motion control in PMSM applications.

Thesis Supervisor: Ton Duc Do
Title: Associate Professor

Acknowledgments

I want to express my sincere gratitude to my supervisor Professor Ton Duc Do for his guidance, willingness to help and teach. Also, i am thankful to Professor Matteo Rubagotti for his help during my research.

I am grateful to the members of my research team from PCMC lab, especially, Yussuf Shakhin and Aizaz Ali Khan for being supportive and helping me during my research path. Special thanks to Postdoctoral Scholar Dr. Ahmad Alhassan for teaching me the foundations of Sliding Mode Controller and Disturbance Observer design.

I appreciate the support from Nazarbayev University, its faculty and professors for their support and effort.

Lastly, I am grateful for my parents for their encouragement, support and love throughout my academic journey.

Contents

List of Figures

List of Tables

Chapter 1

Introduction

Permanent Magnet Synchronous Machines (PMSMs) have become vital since their emergence in the 1970s. It was a product of earlier machine designs, PMSMs combine the advantages of permanent magnet DC machines, line-start PM machines, and power converter-supplied induction machines, which makes them a competent competitor against induction motors as the workhorse of modern industry [5]. Their inherent characteristics, such as high efficiency, compact size, and superior performance, are the key factors which make them indispensable in numerous industrial and high-performance applications. However, the nonlinear dynamics of PMSMs, coupled with external disturbances and uncertainties, create significant challenges in achieving precise and reliable control [7, 8].

Among various control strategies, Variable Structure Control (VSC) with Sliding Mode Control (SMC) stands out for its robustness and adaptability. Introduced in the early 1950s in the Soviet Union by Emelyanov and further developed by researchers such as Utkin and Itkis [1], SMC has garnered widespread interest due to

its unique ability to handle complex control challenges. SMC has been successfully applied to a wide range of systems, including nonlinear systems, multi-input multi-output (MIMO) systems, discrete-time models, large-scale and infinite-dimensional systems, and stochastic systems [2].

The key feature of SMC is its insensitivity to parametric uncertainties and external disturbances during the sliding mode phase [3]. This robustness is achieved by using a high-speed switching control law to drive the nonlinear plant's state trajectory onto a predefined surface, known as the sliding or switching surface, and maintaining the trajectory on this surface thereafter [4]. This dynamic control structure not only provides flexibility in designing the system's behavior but also ensures that the closed-loop response becomes entirely insensitive to a specific class of uncertainties [3]. Furthermore, SMC's ability to specify performance directly makes it a particularly attractive approach for control system design [1].

Despite the strengths of SMC, the intrinsic nonlinear dynamics and disturbance-prone nature of PMSMs necessitate the incorporation of additional strategies to enhance control precision. Disturbances in PMSM systems arise from factors such as fluctuating voltage and frequency, changes in load, temperature variations affecting mechanical properties, and external electrical noise [6]. These disturbances not only degrade system performance but can also cause instability, particularly when relying solely on vector control methods [6].

To address these challenges, Disturbance Observer-Based Control (DOB) offers a promising solution. By observing and compensating for disturbances, DOB enhances performance optimization, improves efficiency, and ensures reliable operation

of PMSMs. Moreover, DOB facilitates condition monitoring, enabling proactive maintenance and reducing the risk of major failures. The integration of DOB with SMC is expected to create a robust control framework capable of addressing the challenges inherent to PMSM systems.

This thesis focuses on designing an SMC-based control framework for PMSMs and evaluating its performance with and without the incorporation of DOB. The objective is to highlight the advantages of combining SMC's robustness with DOB's disturbance compensation capabilities, ensuring precise, efficient, and reliable control of PMSM systems under various operational conditions.

The importance of this research is to address the critical challenges of controlling Permanent Magnet Synchronous Machines (PMSMs), which are significant to modern industrial and high-performance applications. As industries increasingly demand high precision, efficiency, and reliability, developing advanced control strategies that deal with disturbances and uncertainties becomes important. Sliding Mode Control (SMC) is a well-established technique known for its robustness against uncertainties, but its practical implementation often faces challenges related to chattering and sensitivity to unmodeled dynamics. By integrating DOB mechanism, this work aims to enhance the performance of SMC, providing a more stable and resilient control solution for PMSMs.

Moreover, this research contributes to advancing the state-of-the-art in control systems by exploring the synergies between SMC and DOB in the context of nonlinear systems. The findings have the potential to extend beyond PMSMs, influencing the design and optimization of controllers for a wide range of applications, such as

robotics, renewable energy systems, and electric vehicles. By systematically comparing the performance of PMSM systems with and without DOB, this work also provides valuable insights into the practical benefits of disturbance observation and compensation, guiding future innovations in the field.

1.1 Literature Review

1.1.1 Sensorless Control Techniques

PMSMs are widely recognized for their high power density, efficiency, and rapid dynamic response, making them a staple in various applications ranging from household appliances to transportation and aviation. However, traditional control methods relying on shaft encoders for position detection introduce issues such as increased cost, volume, and reduced reliability. Sensorless control methods address these challenges by eliminating the encoder, leveraging techniques like initial position detection methods, low-speed control strategies, and high-speed strategies. These approaches enhance robustness and reliability while maintaining high control precision, making them increasingly popular in PMSM applications [9, 10].

1.1.2 Comparative Analysis of Field-Oriented Control and Direct Torque Control

Field-Oriented Control (FOC) and Direct Torque Control (DTC) are among the most established strategies for PMSM control. FOC decouples the control of torque and flux through d-q axis transformations, enabling precise control analogous to that of DC motors. This method ensures low torque ripple and high dynamic performance

but requires accurate rotor position detection [10, 11]. In contrast, DTC offers faster dynamic response and simplified implementation by directly controlling the motor's torque and flux using a predefined switching table. However, it is prone to higher torque ripples and requires computational resources to manage switching vectors [11].

1.1.3 Sliding Mode Control for PMSMs

SMC has gained attention for its robustness against uncertainties and external disturbances, characteristics critical for high-performance PMSM drives. SMC ensures insensitivity to parameter variations and disturbances by driving system states to a user-defined sliding surface. However, traditional SMC faces challenges such as chattering, which can degrade performance [11, 13]. To mitigate these issues, advanced second-order sliding mode (SOSM) techniques have been developed, which reduce chattering while maintaining robustness. SOSM methods, particularly when integrated with disturbance observers, show significant improvements in performance [13].

1.1.4 Integration of Disturbance Observers in PMSM Control

DOBs play a pivotal role in enhancing the robustness of PMSM control strategies by accurately estimating and compensating for disturbances such as torque ripple, parameter variations, and external noise. The integration of iterative learning control (ILC) with DOBs has further improved disturbance compensation, especially for periodic disturbances like torque ripples. Recent advancements in ILC-DOB methods demonstrate significant improvements in both steady-state and dynamic performance, particularly in reducing torque ripple and enhancing low-speed operation [19, 13].

1.1.5 Advanced Control Strategies

Recent studies explore composite control approaches combining SOSM and DOB techniques to address mismatched disturbances in PMSM drives. These strategies not only minimize torque ripple but also enhance overall system robustness and reduce control effort. For instance, a novel composite SOSM control algorithm with ILC-DOB has shown exceptional capabilities in dealing with low-speed instability issues and improving transient response [13].

The reviewed literature underscores the importance of combining robust control techniques like SMC with advanced disturbance observation methods to address the challenges in PMSM control. While traditional methods like FOC and DTC remain relevant, the integration of SOSM and ILC-DOB marks a significant step forward in enhancing the precision, reliability, and efficiency of PMSM drives. This research builds upon these advancements, aiming to optimize PMSM performance through a synergistic integration of SMC and DOB methodologies.

1.2 Problem

While significant progress has been made in the control of PMSMs, several gaps remain. First, traditional control strategies such as FOC and DTC often struggle with robustness against parameter variations and external disturbances, particularly at low speeds [9, 11]. Although SMC offers robustness to uncertainties, it suffers from chattering effects, which can negatively impact system performance and actuator longevity. Recent advances, such as SOSM controllers, partially address these issues, but often at the cost of increased computational complexity [13]. Furthermore, the

integration of DOBs with SMC has shown promise in mitigating torque ripple and external disturbances, however, these approaches rely on precise system modeling and may falter under conditions of high model uncertainty or abrupt load changes [13]. Additionally, while iterative learning-based DOBs have demonstrated improved periodic disturbance rejection, their applicability in real-time systems with varying operating conditions remains underexplored [13]. Lastly, limited research focuses on experimentally validating these advanced control strategies in diverse practical scenarios, such as mismatched disturbances or varying load profiles, highlighting the need for more comprehensive experimental studies to bridge the gap between theory and application. This work seeks to address these challenges by developing a robust control framework that leverages the strengths of SMC and DOB while addressing their limitations.

1.3 Objective

PMSM is a critical component in modern high-performance systems because of its high efficiency, power density, and dynamic response capabilities. However, precise control of PMSMs is challenging due to their non-linear dynamics, sensitivity to parameter variations, and susceptibility to disturbances such as torque ripple, external noise, and load variations. Traditional control methods, such as FOC and DTC, often face limitations in robustness, especially under low-speed operations or mismatched disturbances. Although SMC offers robust control properties, its practical implementation suffers from chattering, which can degrade system performance and hardware reliability. Recent advances, such as DOB, have demonstrated potential in mitigating external disturbances and improving control precision. However, existing DOB approaches often require accurate system models, limiting their applicability

in systems with high uncertainties or dynamic environments. Moreover, the integration of SMC and DOB has shown promise, but requires further exploration to optimize performance under practical conditions, such as varying loads and parameter uncertainties. To address these challenges, this research aims to develop a robust control framework for PMSM systems by integrating SMC and DOB techniques. The proposed approach will:

1. Leverage SMC to provide robustness against parametric uncertainties and external disturbances while addressing chattering issues using second-order sliding-mode techniques.

2. Incorporate DOB to enhance disturbance rejection capabilities, particularly for periodic disturbances such as torque ripple, and improve overall system robustness.

3. Compare the performance of the PMSM system with and without DOB integration under various operating conditions, focusing on key metrics such as torque ripple suppression, transient response, and steady-state accuracy.

The problem is thus formulated as designing and evaluating a control strategy that integrates SMC and DOB to address the limitations of existing PMSM control methods, ensuring enhanced precision, robustness, and efficiency in practical applications.

Chapter 2

Permanent Magnet Synchronous Motor Working principle, Control Strategies

Permanent magnet synchronous machines were developed in the 1970s as the result of improvement of older machines such as PM DC machines, line-start PM machines, and power converter-supplied induction machines. Therefore, PMS machines contain the advantages of these machines which allows them to compete with induction motors in modern industry. In general, PMSM show considerably higher efficiency compared to the induction motors of the same rating [5]. The advantages that PMSM proposes are high power and torque densities, wide speed regulation [13], environmentally friendly [5] and a compact structure [3] is the reason why it is used in a wide variety of fields such as aerospace, rail transportation, new energy, and others [13].

2.1 Working Principle

The working principle of PMSM is based on the induced magnetic field. The primary parts of the motor that allow it to work are stator and rotor. The stator is a stationary part that generates rotating magnetic fields due to three-phase AC current directed to electromagnetic coils. The permanent magnet located in a rotor part under effect of the magnetic field produced by the stator creates a torque resulting in rotation of the moving rotor part [5]. The classification of types of PMSM are basically done depending on the location of the magnet. According to this, the PMSM type with the magnet placed on the surface of the rotor is called surface-mounted PMSM, while the motor with the magnet located in the inner side of the rotor is called interior PMSM.

2.2 Control Strategies

The traditional approach of controlling PMSM is the cascade control structure with inner current and outer speed loops with two PI controllers, where the speed loop takes the reference speed as an input and provides the Id and Iq reference values to the inner loop [14]. The non-cascade control structure with the single loop has become quite popular recently [16]. The single loop structure has its own advantages over the traditional control structure as a simple form and less parameters needed to be controlled [16]. Despite these advantages, single loop structure means that Iq becomes the state of the system and will no longer be controllable as in case of cascade control structure by the reference signal from outer loop.

There were applied various speed regulation strategies to ensure swift and smooth convergence to the set value. Among them, optimal control stands out because it

guarantees that both steady state and dynamic responses are high level [15]. However, there is a problem of nonlinear behavior of PMSM which requires solving Hamilton–Jacobi–Bellman (HJB) equations [17]. The proposed solution was to implement Adaptive Dynamic Programming with 2 Neural Networks instead of solving nonlinear HJB equations and reject the mismatched disturbances using Disturbance Observer (DOB) [18].

The other advanced method for PMSM tracking performance optimization is applying Sliding Mode Control (SMC). The traditional SMC in a speed loop can only provide asymptotic stability [19]. The main problem of SMC is chattering which can be solved by introducing High Order Sliding Mode (HOSM) with Super Twisting Algorithm (STA) [20]. Another method is a combination of Super Twisting Sliding Mode (STSM) aided with Generalized Proportional Integral Observer which is more efficient than STSM in terms of dealing with unwanted dynamic response due to high switching gain [21].

The use of advanced control strategies is required to achieve high dynamic performance in PM motors equires . Among these, *Field-Oriented Control* (FOC) has emerged as a highly effective approach. By utilizing mathematical transformations, it becomes possible to decouple the torque generation and magnetization processes within the motor. This decoupled control is what defines FOC. Through the vector manipulation of voltages and currents, the magnetic fields inside the motor are spatially aligned, a concept which is called “field orientation." The main function of an FOC controller is to maintain a consistent electrical angle between the stator and rotor field vectors [5, 26, 27, 28].

FOC operates by managing the stator currents as a vector quantity. This is achieved by transforming a three-phase time-dependent model into a two-axis time-invariant representation using the direct-quadrature (d-q) transformation. This model

requires two steady inputs: the torque-generating component aligned with the q-axis, and the flux-producing component orthogonal to it on the d-axis [29]. The projection-based transformation allows for the immediate regulation of electrical variables, ensuring accurate control during both steady-state and transient responses, despite the limitations due to mathematical bandwidth of the system.

Compared to conventional motor control strategies, FOC offers several considerable benefits. Most notably, it simplifies a complex and coupled AC motor model into a linear representation that separates torque and flux control, akin to how DC motors are managed. This separation leads to rapid dynamic response and strong performance under transient and steady-state conditions. FOC also delivers high starting torque while requiring relatively low current, which improves system efficiency. In addition, it supports a wide speed range making it a preferred method in many PM motor applications. Therefore, this thesis utilizes the FOC strategy for the speed control of a PMSM.

FOC involves a series of transformations across three reference frames: the stator frame (a, b, c), the stationary orthogonal frame (α, β), and the rotor frame (d, q) [5]. The stator frame consists of three coplanar phases spaced 120° apart. The (α, β) frame uses orthogonal axes spaced 90° apart, while lying in the same plane. The rotor reference frame is defined by two axes: the d-axis, which aligns with the rotor's magnetic flux and poles, and the q-axis, which is perpendicular to it. These transformations are fundamental to enabling separate control of torque and flux, therefore, supporting efficient operation, fast dynamic response, and strong transient and steady-state behavior.

As shown in Figure 2-1, the transformation process includes the decoupling of the stator currents into torque- and flux-producing components. These components are then individually regulated using PID controllers. Finally, an inverse transformation

converts the control outputs back into the stator frame for application to the motor.

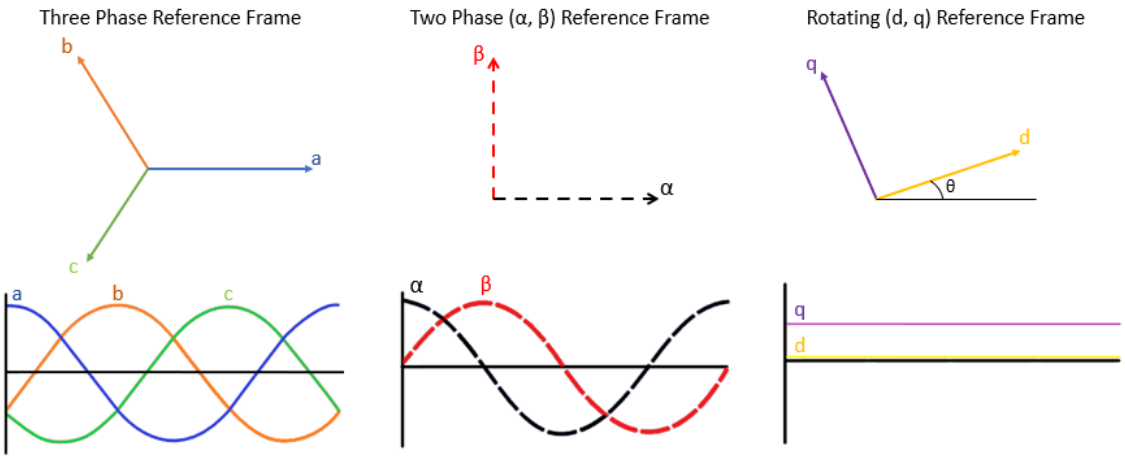

Figure 2-1: Reference Frames

Field-Oriented Control (FOC) operates by analyzing the torque and flux components of a motor within the rotating d–q reference frame. Because the stator current measurements originate in a three-phase, time-varying reference frame, a transformation to a two-axis d–q system aligned with the rotor is necessary. This transformation is performed in two primary stages, as illustrated in Figure 2-2.

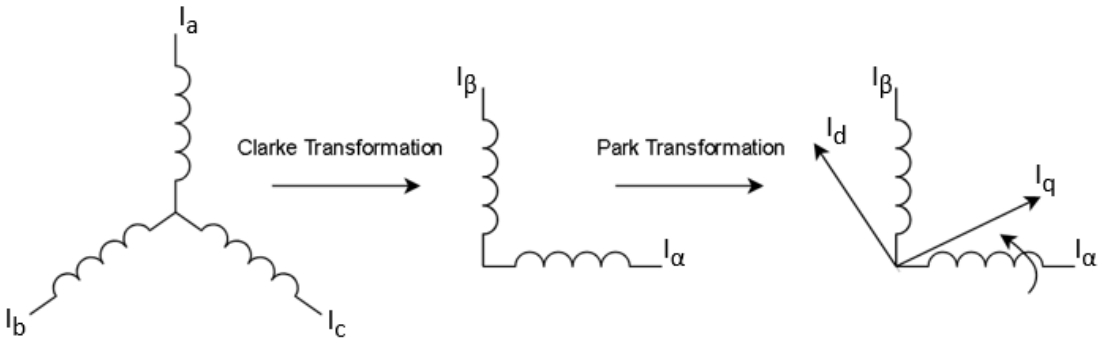

Figure 2-2: Transformation from a-b-c to d-q frame

The first stage involves converting the three-phase stator currents into a stationary two-axis (α, β) frame using the Clarke transformation, also known as the α–β transform. This is done by applying a transformation matrix that projects the three-phase signals onto orthogonal axes aligned with the stator. The Clarke transformation is given by the following matrix equation [30]:

$$\begin{bmatrix} \alpha \\ \beta \\ 0 \end{bmatrix} = \frac{2}{3} \begin{bmatrix} 1 & -\frac{1}{2} & -\frac{1}{2} \\ 0 & \frac{\sqrt{3}}{2} & -\frac{\sqrt{3}}{2} \\ \frac{1}{2} & \frac{1}{2} & \frac{1}{2} \end{bmatrix} \begin{bmatrix} a \\ b \\ c \end{bmatrix} \tag{2.1}$$

Once transformed, the α and β components are rotated into the d–q frame using the Park transformation, which aligns with the rotor's magnetic field at an angle θ. The d–q frame is widely used for control and analysis of electric machines due to its ability to align control with the machine's torque generation capabilities. Since the maximum torque in such machines is orthogonal to the magnetic flux, aligning the q-axis with the torque and the d-axis with the flux is ideal. Regulating these components enables optimized control. Specifically, the d-current, which does not contribute to torque, is minimized, while the q-current, which has a direct linear relation to torque, is adjusted to regulate motor performance.

The Park transformation is defined by [30]:

$$\begin{bmatrix} d \\ q \\ 0 \end{bmatrix} = \begin{bmatrix} \cos\theta & \sin\theta & 0 \\ -\sin\theta & \cos\theta & 0 \\ 0 & 0 & 1 \end{bmatrix} \begin{bmatrix} \alpha \\ \beta \\ 0 \end{bmatrix} \tag{2.2}$$

The fundamental purpose of vector control (VC) is to achieve independent control of torque and flux in AC motors—an approach similar to that used in DC motor control. By decoupling the d- and q-axes, the system allows torque to be controlled

via i_q and flux via i_d in permanent magnet (PM) motors. Figure 2-3 illustrates a typical vector-controlled PMSM drive system utilizing d–q current controllers.

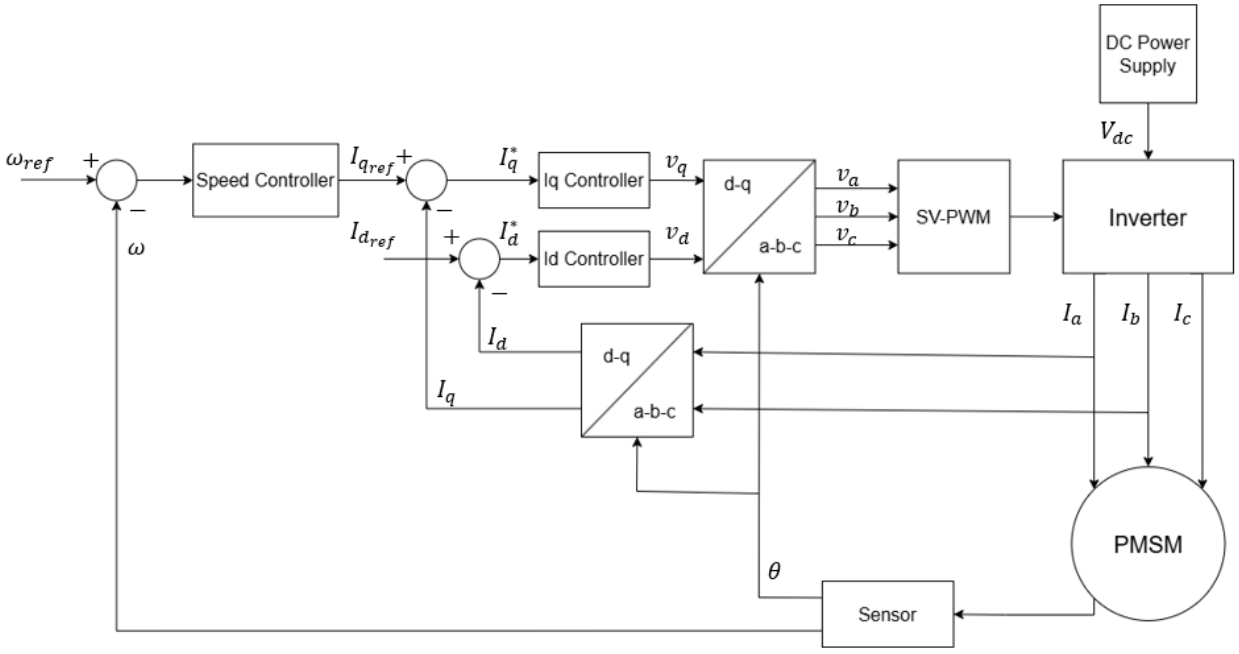

Figure 2-3: Vector-controlled PMSM block diagram [30]

This system receives two current references—i_d and i_q—which are compared to the feedback currents from sensors. The resulting current errors are processed by controllers, producing voltage commands v_d and v_q. These voltages are then transformed back to the three-phase stator reference frame through inverse transformations, using the rotor position angle θ.

Phase currents (i_a, i_b, i_c) measured by sensors are transformed into the i_d and i_q frame as a feedback, while the calculated voltages (v_d, v_q) are transformed back into (v_a, v_b, v_c) to drive the inverter. The rotor position θ—often measured using an encoder—is essential for these transformations. A PWM system converts the voltage commands into switching signals for the inverter, which in turn converts DC input

power into three-phase AC power to drive the motor.

This control system provides consistent torque output and regulates the rotor speed following the reference speed. The actual speed is derived by differentiating the rotor position, and the error between the reference and actual speed is used by the speed controller to generate the i_q reference current for precise regulation.

Chapter 3

Sliding mode control & Disturbance Observer

3.1 (

SMC) Sliding Mode Control (SMC) is a nonlinear control technique which is the crucial part of robust control systems design. SMC was developed to tackle one of the most persistent problems in control engineering: maintaining desired system performance in the presence of uncertainties, disturbances, and unmodeled dynamics based on the theory of Variable Structure Systems (VSS).Vss was invented in the Soviet Union in the mid-20th century. The idea is to switch between different control structures depending on the current state of the system. This means that the sliding mode acts as a dynamic regime in which the system's behavior becomes invariant to certain types of disturbances [24].

The main idea of SMC is the concept of sliding surface. The sliding surface is a mathematical function defined based on the system's state variables. When the

system state reaches this surface, it is constrained to move along it by a discontinuous control law. This is called sliding mode and it provides useful characteristics such as reduced-order dynamics and insensitivity to matched uncertainties and disturbances. The control design process is typically divided into two steps: first, the sliding surface is crafted such that the dynamics restricted to this surface fulfill the control objectives; second, a switching control law is designed to ensure that the system trajectory reaches the sliding surface in finite time and remains on it despite perturbations [22].

The practical relevance of SMC comes from its robustness properties. Since the control law compensates for modeling inaccuracies and external disturbances systematically, it is highly effective in applications where precision and stability are required under uncertain conditions such as electromechanical systems, power electronics, robotics, and aerospace engineering. Examples of successful SMC implementations are DC/DC converters, induction motor drives, robotic manipulators, and quadrotor drones [23]. Its ability to deliver finite-time convergence and maintain performance under a wide range of conditions makes it particularly attractive in modern engineering systems.

Despite its advantages, the standard SMC has its own limitations. The most critical of these is the chattering effect, a high-frequency oscillation around the sliding surface caused by the discontinuous switching of the control input. Chattering can lead to wear and tear in mechanical systems and may excite unmodeled high-frequency dynamics, posing serious implementation challenges. Various strategies have been proposed to solve this issue, such as boundary layer techniques, quasi-sliding modes, and the Higher-Order Sliding Mode (HOSM) control. HOSM methods aim to maintain the robustness of standard SMC while smoothing out the control signal by acting on higher derivatives of the sliding variable, therefore reducing or

even eliminating chattering [22].

An additional advantage of HOSM control is its enhanced tracking and disturbance rejection capabilities, especially for systems with relative degrees greater than one. In these cases, standard SMC design becomes difficult or even impossible. By ensuring that the sliding variable and its derivatives converge to zero, HOSM provides a systematic approach for robust control of complex dynamic systems. This makes them suitable for precision-critical applications such as insulin delivery in biomedical systems, satellite formation control, and fault-tolerant robotics [22].

The evolution of SMC from a standard first-order formulations to modern higher-order types has transformed it into a robust and versatile control method. Its theoretical foundation and practical efficiency have resulted in further research interest and widespread use in various domains. As new technologies emerge, particularly in cyber-physical systems and autonomous platforms, the relevance of sliding mode control is only expected to grow.

3.2 Review of State-of-the-Art SMC Applications to PMSM Speed Control

Recent developments in SMC have shown strong potential for improving the robustness and performance of speed control in PMSMs. It is necessary to introduce advanced control strategies beyond traditional PI or PID control due to the nonlinear behavior of PMSMs, strong parameter coupling and sensitivity to load torque disturbances.

Zaihidee et al. [33] presented a comprehensive review of various enhancements made to SMC for PMSMs, including integral SMC (ISMC), fractional-order SMC

(FOSMC), and terminal SMC (TSMC). The study emphasized the need for high tracking precision and robust disturbance rejection in modern PMSM applications such as robotics and electric vehicles. ISMC was noted for its capability to eliminate the reaching phase and maintain robustness throughout the entire response, while FOSMC and TSMC offered superior chattering reduction and faster convergence respectively.

Zhao and Dong [34] proposed a novel second-order SMC approach for the phase-q current control loop of PMSMs, which incorporated a low-pass filter to attenuate chattering. They derived a modified SMC law from a second-order model that includes the counter electromotive force (CEMF) term. Simulation results confirmed that this method effectively compensates disturbances and improves current and speed tracking.

Tran and Jeon [35] introduced a Dual Adaptive Sliding Mode Control (DA-SMC) which combines a robust adaptive sliding mode observer (RASM) with mechanical parameter identification. Their approach significantly reduced parameter estimation errors and improved controller response by improving both reaching law and observer dynamics. The authors demonstrated better convergence and tracking performance in industrial PMSM drives, especially under sudden load changes.

Kumari and Mathew [36] compared several controllers, including PI, PID, SMC, and a hybrid SMC+PID configuration for PMSM vector control. They showed that the integration of SMC improved performance under disturbance and uncertainty. The SMC+PID combination resulted in better transient and steady-state response than conventional methods.

Across these works, one recurring challenge in SMC-based designs is chattering, a high-frequency oscillation near the sliding surface due to discontinuous control laws. Several strategies, such as low-pass filtering, adaptive switching gains, and composite

controllers, were employed to mitigate this issue without compromising robustness.

The next section contains the detailed SMC controller analysis [25]

3.2.1 Problem Statement

We examine the behavior of the following single-input control-affine system influenced by both matched and mismatched disturbances:

$$\dot{x} = b(t)(u + \delta_1(t)) + \delta_2(t) \tag{3.1}$$

Here, $x \in \mathbb{R}$ is the system state, and $u \in \mathbb{R}$ is the control input. The time-varying scalar $b(t)$ represents the control gain, which may cross zero, and $\delta_1(t), \delta_2(t)$ are disturbances affecting the system in different ways:

- $\delta_1(t)$ is a *matched disturbance*, entering the system through the same path as the control input.
- $\delta_2(t)$ is a *mismatched disturbance*, acting independently of the control signal.

The core objective is to ensure the stability of the system in (3.1) despite these disturbances, especially when the control gain $b(t)$ is not of constant sign.

subsection*Assumption 1 – Persistence of Excitation (PE) To handle the challenge of the control gain possibly vanishing or changing sign, we impose the following condition:

$$\int_{t_0}^{t} |b(\tau)|\, d\tau \geq \gamma_1(t - t_0) + \gamma_2 \tag{3.2}$$

This *Persistence of Excitation (PE)* condition ensures that, even though $b(t)$ may be zero at some instants, its overall influence over time remains significant. The constants $\gamma_1 > 0$ and $\gamma_2 \in \mathbb{R}$ quantify this excitation.

Remark 1 – Averaged PE Form

From Assumption 3.2, it follows that for any $\bar{\gamma} < \gamma_1$, there exists a time T_0 such that:

$$\frac{1}{T_0} \int_{t_0}^{t_0+T_0} |b(\tau)| \, d\tau \geq \bar{\gamma} \tag{3.3}$$

This means that the average effect of $b(t)$ over any interval of length T_0 can be lower-bounded, reinforcing the excitation condition.

Lemma 2 – Finite-Time Convergence with PE

Consider the nonlinear scalar differential equation:

$$\dot{c}(t) = -\beta(t) \cdot c^{\frac{\alpha+1}{2}}(t), \quad c(t_0) = c_0 > 0, \quad \alpha \in [0, 1) \tag{3.4}$$

where $\beta(t) \geq 0$ satisfies the PE condition. Then, the solution $c(t)$ reaches zero in finite time, uniformly with respect to the initial time t_0.

Settling Time

Define the constant:

$$a_1 = \frac{1-\alpha}{2} \tag{3.5}$$

The settling time $T(t_0, c_0)$, i.e., the time it takes for $c(t)$ to reach zero, is given by:

$$T(t_0, c_0) = \frac{c_0^{a_1}}{a_1 \gamma_1} - \frac{\gamma_2}{\gamma_1} \tag{3.6}$$

This result ensures that $c(t)$ always converges to zero in finite time under the PE condition.

Corollary 3 – Special Case for $\alpha = 1$

In the special case when $\alpha = 1$, the equation becomes linear and its solution is:

$$c(t) = c_0 \cdot \exp\left(-\int_{t_0}^{t} \beta(\tau)\, d\tau\right) \tag{3.7}$$

This describes exponential decay of $c(t)$, implying asymptotic convergence instead of finite-time convergence.

Remark 4 – Relaxation of the PE Condition

While Assumption 3.2 ensures finite-time convergence, it is not strictly necessary. It is sufficient that:

$$\lim_{t\to\infty} \int_{t_0}^{t} |b(\tau)|\, d\tau = \infty \tag{3.8}$$

This relaxed condition guarantees that for any initial state c_0, there exists some time t^* such that:

$$\int_{t_0}^{t^*} |b(\tau)|\, d\tau = \frac{1-\alpha}{2} \cdot {c_0}^{\frac{1-\alpha}{2}} \tag{3.9}$$

which also leads to convergence of the solution.

3.2.2 Case of Matched Disturbances

We now examine the scenario in which the disturbance is matched. This corresponds to the case where $\delta_2(t) \equiv 0$ and $\delta_1(t) = \delta(t)$, meaning the disturbance enters the system through the same channel as the control input. The system equation simplifies

to:

$$\dot{x} = b(t)(u + \delta(t)) \tag{3.10}$$

Assumption 2

The disturbance $\delta(t)$ is assumed to be uniformly bounded:

$$|\delta(t)| \leq \bar{\delta}, \quad \forall t \in \mathbb{R} \tag{3.11}$$

Now consider a family of nonlinear controllers given by:

$$u = -k \lceil b(t) \rfloor_0 \lceil x \rfloor_\alpha, \quad \alpha \in [0, 1] \tag{3.12}$$

Here, the operator $\lceil x \rfloor_\alpha = \text{sign}(x)|x|^\alpha$ defines a generalized sign-power function.

Proposition 1. *Under Assumptions 1 and 2, if* $\alpha \in (0, 1]$ *and* $k > \bar{\delta}$*, then the solutions of* (3.10) *are ultimately bounded. Specifically:*

$$|x(t)| < \varepsilon^{1/\alpha}, \quad \textit{where } \varepsilon = \frac{\bar{\delta}}{k} < 1 \tag{3.13}$$

Proof. Substituting (3.12) into (3.10), we get:

$$\dot{x} = -k|b(t)|\lceil x \rfloor_\alpha + b(t)\delta(t) \tag{3.14}$$

Consider the Lyapunov function:

$$V = \frac{1}{2}x^2 \tag{3.15}$$

Its time derivative is:

$$\dot{V} = -k|b(t)||x|^{\alpha+1} + b(t)\delta(t)x \tag{3.16}$$

If we define $\bar{\delta} = \varepsilon k$, then:

$$\dot{V} \leq -2|b(t)|k(|x|^{\alpha} - \varepsilon) \tag{3.17}$$

This implies that the solutions are bounded within the set $\{|x|^{\alpha} \leq \varepsilon\}$. □

Corollary 1. *If $\delta(t) = 0$ and $\alpha \in [0, 1)$, then under Assumption 1 and for $k > 0$, the origin is uniformly finite-time stable (UFTS).*

Proof. With $\varepsilon = 0$, the Lyapunov derivative becomes:

$$\dot{V} \leq -2|b(t)|k|x|^{\alpha+1} \tag{3.18}$$

This satisfies the finite-time convergence conditions described in Lemma 2. □

Corollary 2. *In the linear case $\alpha = 1$ with $\delta(t) = 0$ and under Assumption 1, the origin is exponentially stable.*

Proof. The Lyapunov derivative simplifies to:

$$\dot{V} \leq -2k|b(t)|V \tag{3.19}$$

Applying Corollary 3 to Lemma 2 yields exponential convergence. □

Corollary 3. *In the discontinuous case $\alpha = 0$, under Assumptions 1 and 2 with $k > \bar{\delta}$, the origin is UFTS.*

Proof. For $\alpha = 0$, the Lyapunov derivative becomes:

$$\dot{V} = -k|b(t)||x| + b(t)x\delta(t) \tag{3.20}$$

We get:

$$\dot{V} \leq -k(1-\varepsilon)|b(t)|V^{1/2}, \quad \text{with } \varepsilon = \frac{\bar{\delta}}{k} < 1 \tag{3.21}$$

Applying Corollary 3 to Lemma 2 yields exponential convergence. □

Corollary 4. *In the discontinuous case $\alpha = 0$, under Assumptions 1 and 2 with $k > \bar{\delta}$, the origin is UFTS.*

Proof. For $\alpha = 0$, the Lyapunov derivative becomes:

$$\dot{V} = -k|b(t)||x| + b(t)x\delta(t) \tag{3.22}$$

We get:

$$\dot{V} \leq -k(1-\varepsilon)|b(t)|V^{1/2}, \quad \text{with } \varepsilon = \frac{\bar{\delta}}{k} < 1 \tag{3.23}$$

This again satisfies the conditions of Lemma 2 for finite-time stability. □

Remark. Only the discontinuous controller ($\alpha = 0$) guarantees exact theoretical compensation of bounded disturbances. Continuous controllers ($\alpha > 0$) achieve practical stability.

3.2.3 Case of Mismatched Disturbances

Now consider the system when only $\delta_2(t)$ is present (mismatched disturbance), i.e., $\delta_1(t) = 0$. The system becomes:

$$\dot{x} = b(t)u + \delta(t) \tag{3.24}$$

We use the same control law as before:

$$u = -k \lceil b(t) \rceil_0 \lceil x \rceil_\alpha, \quad \alpha \in [0, 1] \tag{3.25}$$

Substituting into (3.24) gives:

$$\dot{x} = -k|b(t)| \lceil x \rceil_\alpha + \delta(t) \tag{3.26}$$

Remark. For the disturbance to be considered matched in the context of a zero-crossing control gain, it must be factorizable as:

$$\delta(t) = \varpi(t) b(t) \tag{3.27}$$

In other words, the disturbance must have no effect when $b(t) = 0$.

Proposition 2. *Assume Assumptions 1 and 2 hold, and $\alpha \in (0, 1)$. If:*

$$k = \frac{\psi \bar{\delta}}{\beta}, \quad \beta \in (0, \gamma_1), \quad \psi > 1 \tag{3.28}$$

then the solution $x(t)$ is uniformly ultimately bounded:

$$|x(t)| \leq \left[\left(\frac{1}{\psi} \right)^{\frac{1-\alpha}{\alpha}} - \frac{\bar{\delta}\psi(1-\alpha)\gamma_2}{\beta} \right]^{\frac{1}{1-\alpha}} \tag{3.29}$$

Proof. Using the Lyapunov function $V = |x|$, we get:

$$\dot{V} = \lceil x \rceil_0 \dot{x} = -k|b(t)|V^\alpha + \delta(t)\,\mathrm{sign}(x) \leq -k|b(t)|V^\alpha + \bar{\delta}$$

This allows a two-part analysis:

- Outside the region $\{|x| < (1/\psi)^{1/\alpha}\}$, the decay dominates.
- Inside the region, the bound guarantees uniform ultimate boundedness.

□

Corollary 5. *For $\alpha = 1$, the bound becomes:*

$$|x(t)| \leq \frac{1}{\psi} \exp\left(-\frac{\psi\bar{\delta}\gamma_2}{\beta} \right) \tag{3.30}$$

Corollary 6. *For the discontinuous case $\alpha = 0$, if:*

$$k = \frac{\varepsilon_1 \bar{\delta}}{\gamma_1}, \quad \varepsilon_1 > 1 \tag{3.31}$$

then:

$$|x(t)| \leq -\bar{\delta}\frac{\gamma_2}{\gamma_1} \tag{3.32}$$

Remark. When both matched and mismatched disturbances are present, one can increase k to compensate for the matched disturbances and ensure that the effect of the mismatched disturbances remains bounded.

3.2.4 Controller Design for PMSM Application

Using the controller proposed above, the designed SMC controller equations are the following:

$$e = \omega - \omega_{\text{ref}} \tag{3.33}$$

$$T_m = -k \left\lceil \frac{1}{J} \right\rfloor_0 \lceil e \rceil_\alpha \tag{3.34}$$

$$T_m = -k \lceil e \rceil_\alpha \tag{3.35}$$

where the system equations are:

$$\dot{\omega} = \frac{1}{J}(T_m - \tau_d) \tag{3.36}$$

$$\tau_d = T_L + B_m\omega + \text{sign}(\omega)N \tag{3.37}$$

Here, J represents the moment of inertia of the motor, and τ_d denotes the total disturbance torque acting on the system. The terms B_m and N refer to the viscous and static friction coefficients, respectively. The total disturbance torque τ_d accounts for the external load torque T_L as well as the internal frictional torques generated by both viscous damping and static friction within the PMSM.

3.3 DOB Analysis

DOB is a robust control technique that improves the performance of motion control systems by estimating and compensating for external disturbances and model uncertainties. DOB introduces an inner feedback loop that estimates disturbances based on a nominal model and feeds them back to reject their effect, therefore achieving robustness against model inaccuracies and external disturbances [31]. This structure allows the outer-loop controller to focus solely on nominal system dynamics, forming what is known as a two-degrees-of-freedom (2-DOF) control scheme.

The typical DOB configuration comprises a low-pass filter (LPF) and the inverse of a nominal plant model. Although the LPF ensures causality, it also introduces limitations on performance and robustness. Especially, the LPF's bandwidth must be carefully selected to balance between disturbance rejection and noise sensitivity [32]. Bode and Poisson integral formulas have been used to derive these bandwidth constraints [31].

Although continuous-time analysis offers theoretical clarity, practical systems often require discrete-time (DT) DOB implementations. Discretization methods, such as Euler and Tustin, greatly affect system behavior in the DT domain. Properly designed DOB provides an effective and general-purpose method to improve disturbance rejection, ensure stability, and optimize tracking performance in precision motion systems [32].

The sensitivity and complementary sensitivity functions can be obtained based on Figure 3-2. These equations show the effect of G_b and α and importance of proper DOB design.

$$S(s) = \frac{PQ + P^{-1}(1-Q)}{PQ + P^{-1}(1-Q) + PP^{-1}C} \tag{3.38}$$

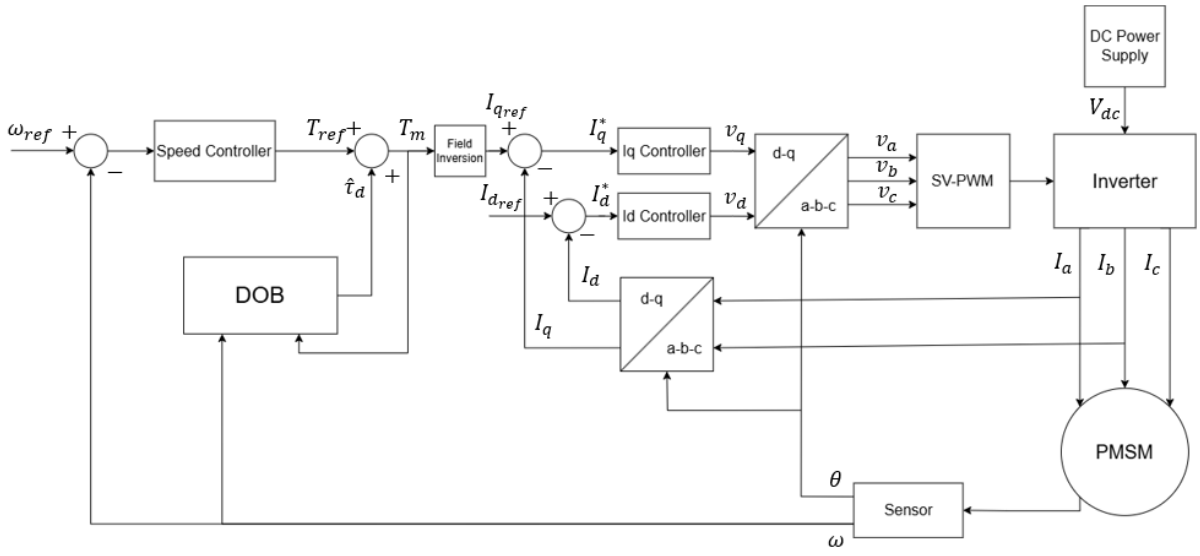

Figure 3-1: Vector-controlled PMSM & DOB block diagram

$$T(s) = \frac{PP^{-1}C}{PQ + P^{-1}(1-Q) + PP^{-1}C} \tag{3.39}$$

where:

$$P(s) = \frac{1}{Js} \tag{3.40}$$

$$Q(s) = \frac{G_b}{s + G_b} \tag{3.41}$$

The sliding mode control law was previously defined as:

$$T_m = -k \lceil e \rceil_\alpha \tag{3.42}$$

where $e = \omega - \omega_{\text{ref}}$ denotes the tracking error, $k > 0$ is the control gain, and the

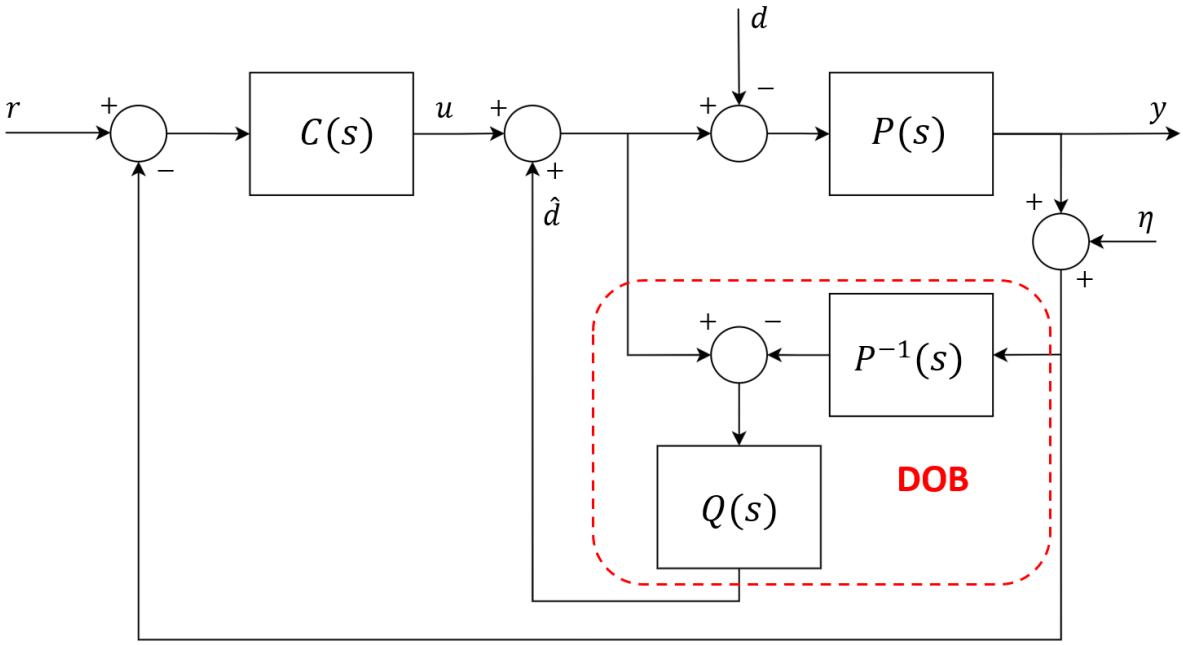

Figure 3-2: DOB block diagram

notation $\lceil e \rceil_\alpha$ denotes the sign-power function:

$$\lceil e \rceil_\alpha = \text{sign}(e)|e|^\alpha$$

In the case where $\alpha = 1$, the control law becomes a linear function of the error:

$$T_m = -ke \tag{3.43}$$

This simplification eliminates the nonlinearity and allows the control input to be treated as a standard proportional feedback.

Taking the Laplace transform of both sides (assuming zero initial conditions), we

obtain the transfer function of the controller:

$$C(s) = \frac{T_m(s)}{e(s)} = k \tag{3.44}$$

This presents the sliding mode controller in the $\alpha = 1$ case as a simple proportional controller with gain k. It should be noted that this is a continuous approximation.

The DOB sensitivity and complementary sensitivity functions are the following:

$$S_d = \frac{s}{s + \alpha G_b} \tag{3.45}$$

$$T_d = \frac{\alpha G_b}{s + \alpha G_b} \tag{3.46}$$

In the following, the frequency characteristics of these equations are provided.

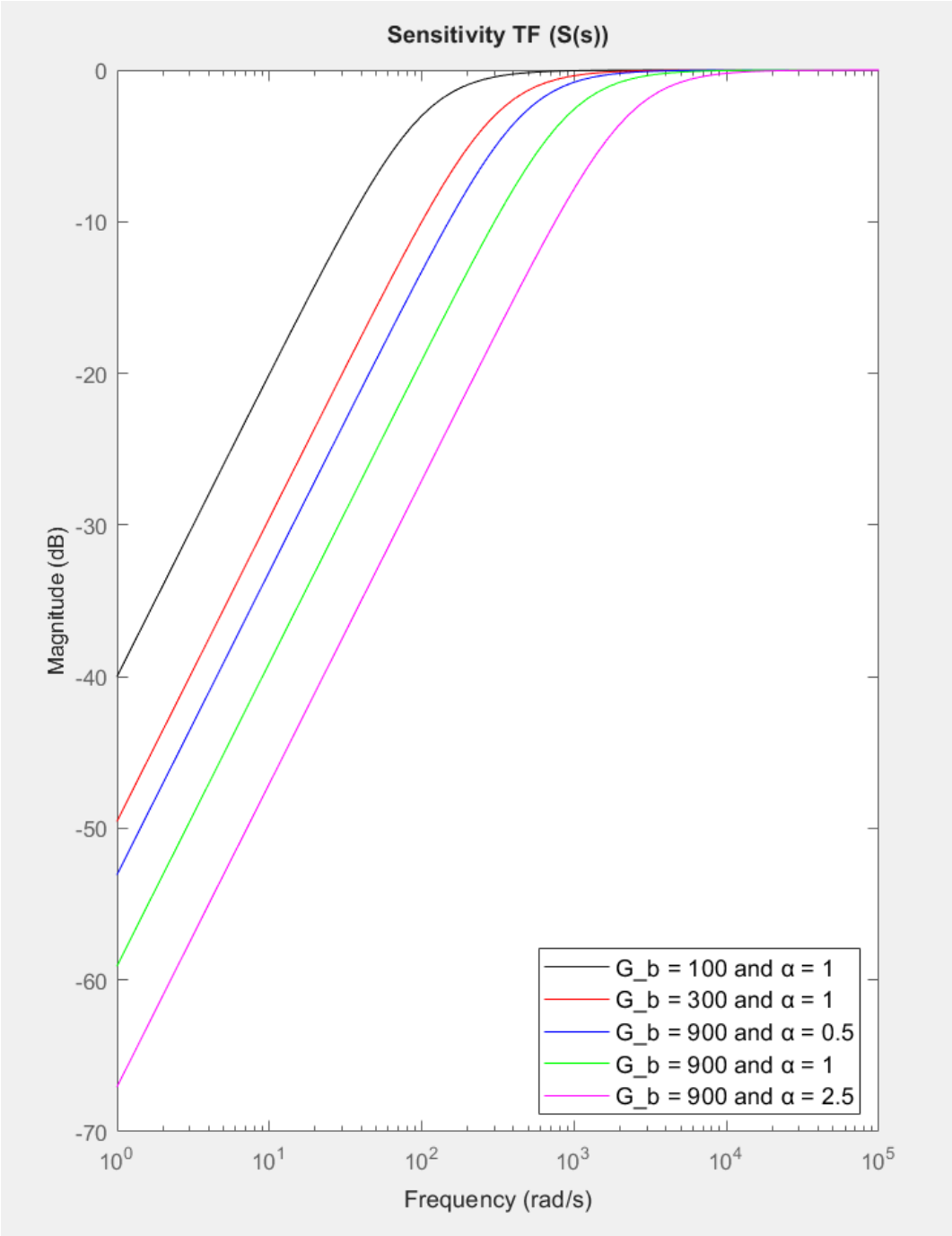

Figure 3-3: Sensitivity transfer function

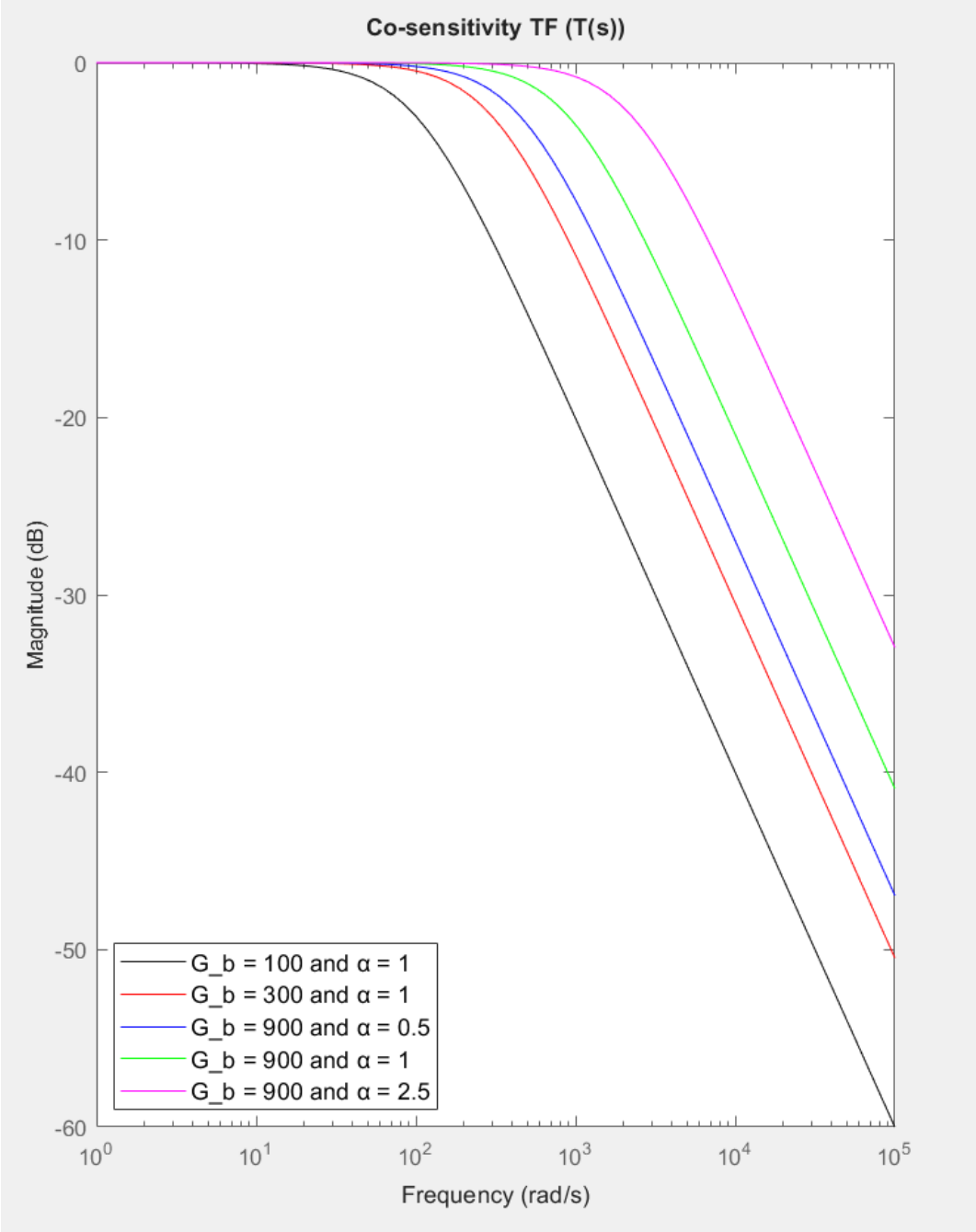

Figure 3-4: Complementary sensitivity transfer function

Increasing α and G_b increases the observer's effective frequency bandwidth and enhances its robustness, as illustrated in the frequency response of the sensitivity transfer function of the DOB, shown in Figures 3-3 and 3-4. Motor disturbances typically span a wide frequency spectrum, with high-frequency components being particularly problematic. As demonstrated in the figure, higher values of the design parameters lead to improved attenuation of disturbances across the full frequency range.

Chapter 4

Experimental Results and Discussion

In order to conduct the experiment, a 300W PMSM from Power Conversion and Motion Control (PCMC) lab was used. Below the motor parameters are listed in the table and its visual representation are presented. The model obtained so far was

Table 4.1: PMSM Parameters

Parameter	**Value**
Pole Pair	4
Rated Speed (N_s)	2000 RPM
Rated Torque (T_m)	0.97 N-m
Peak Torque (T_{peak})	4 N-m
Inductance d-axis (L_d)	0.0043 H
Inductance q-axis (L_q)	0.0043 H
PM Flux	0.0623 Wb
Phase-phase Winding Resistance	4.74 Ω
Max Current (I_{peak})	12 A

compared with the PI controller proposed by the LN system itself with a DOB. The performance was tested based on two types of experiments. The first experiment is aimed to test the performance of the controller for the application of the load at a constant speed. The second experiment focuses on making a speed change while

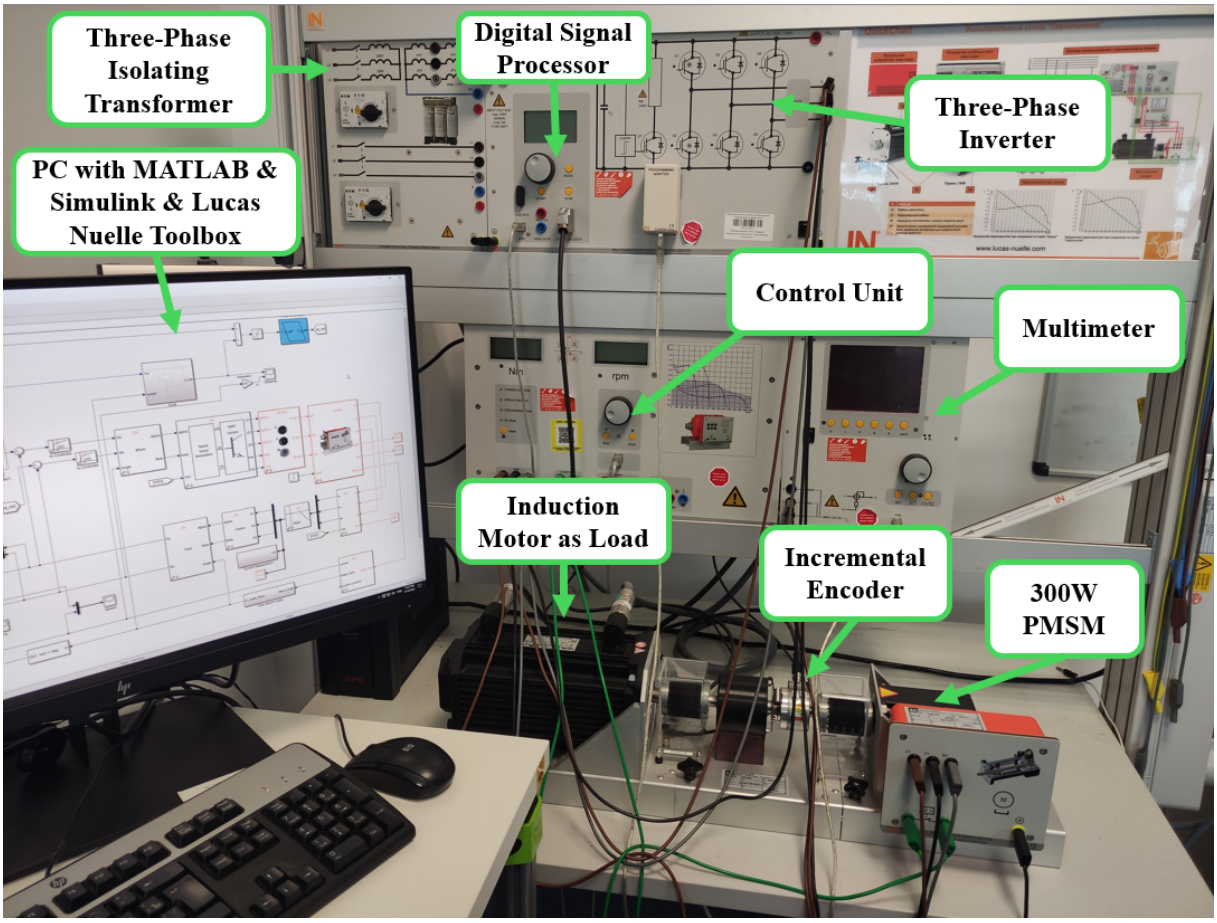

Figure 4-1: PMSM setup representation with notations

the load is applied. During these experiments the speed tracking response, Iq and Id currents and disturbance estimation from the DOB are compared between two models mentioned above.

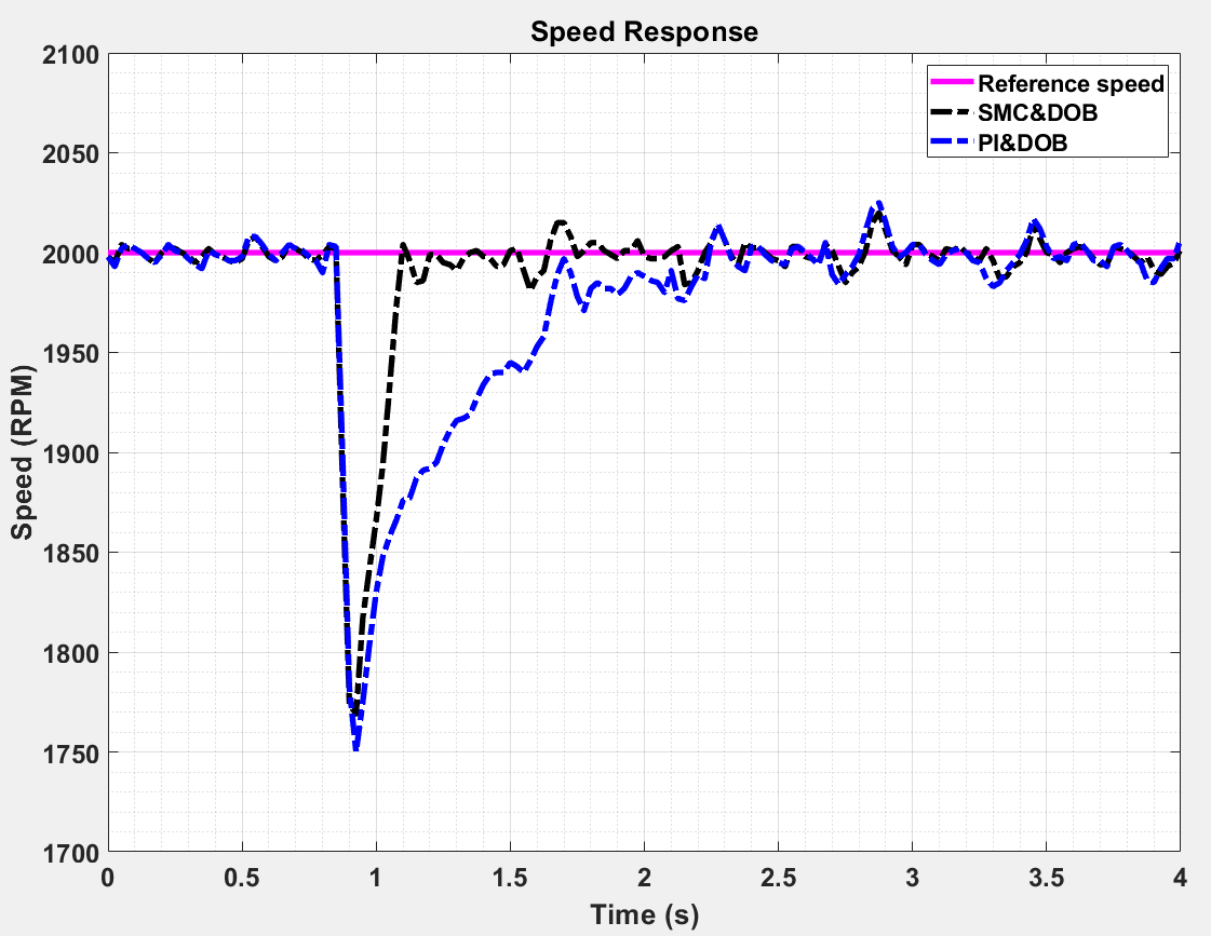

Figure 4-2: Load application experiment, speed response comparison

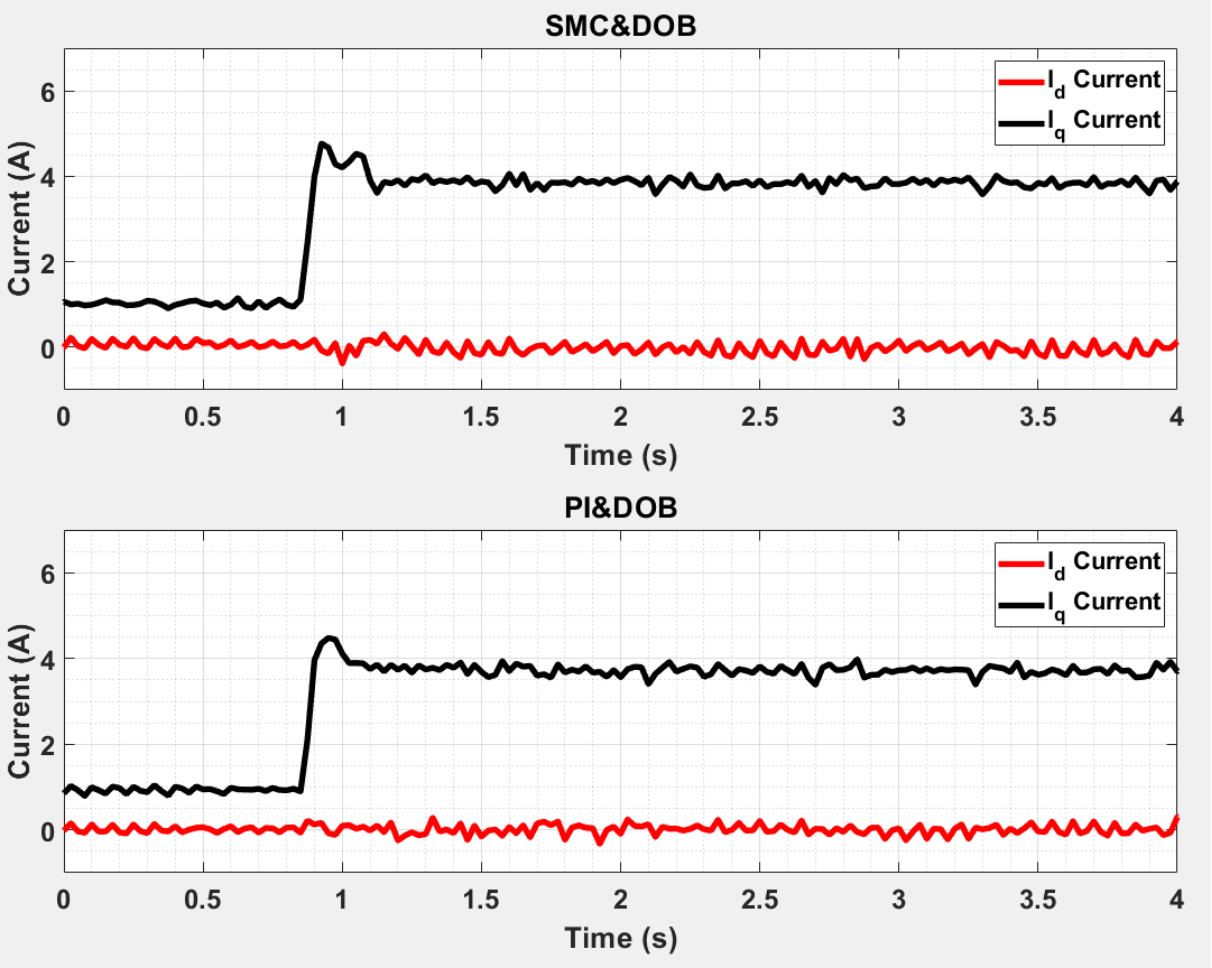

Figure 4-3: Load application experiment, current response comparison

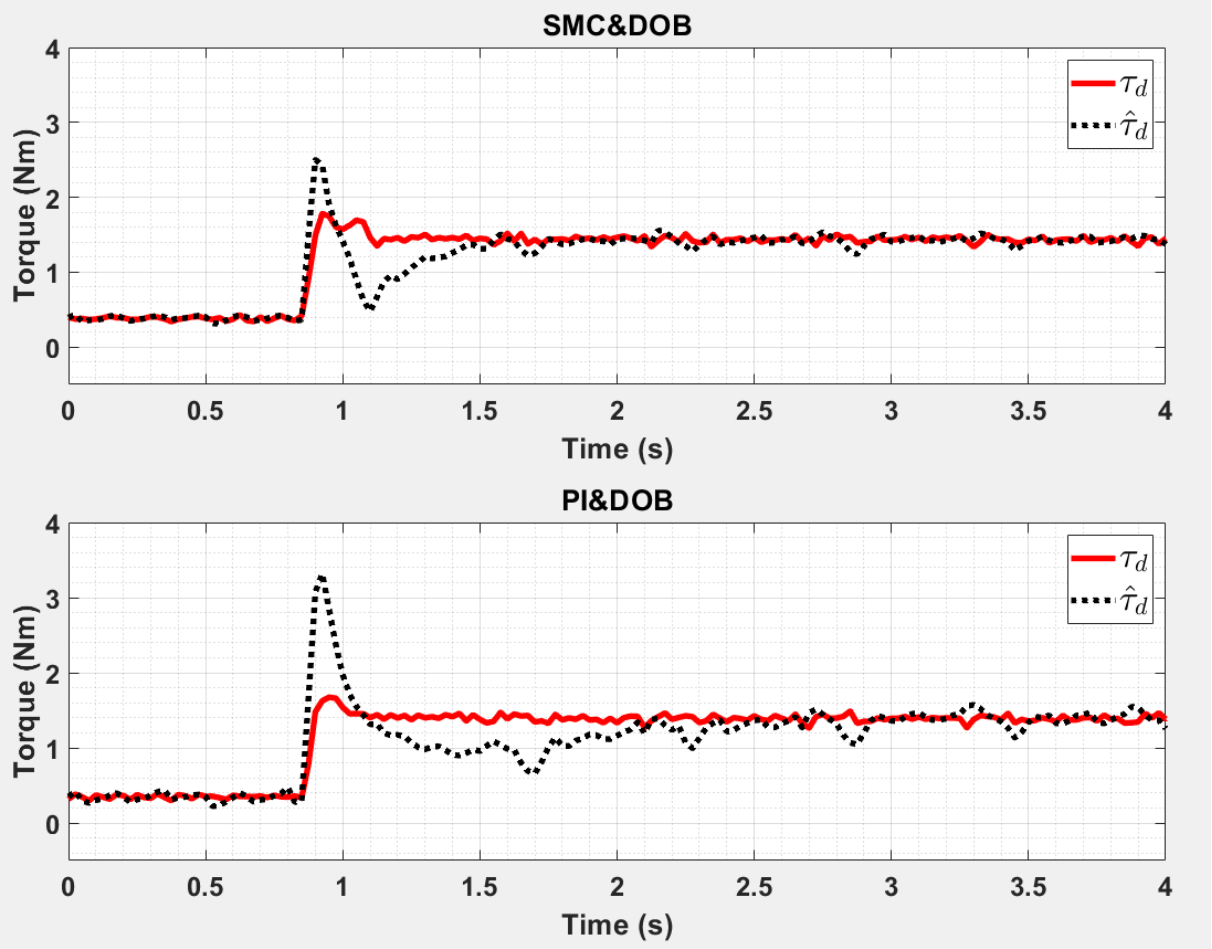

Figure 4-4: Load application experiment, disturbance estimation comparison

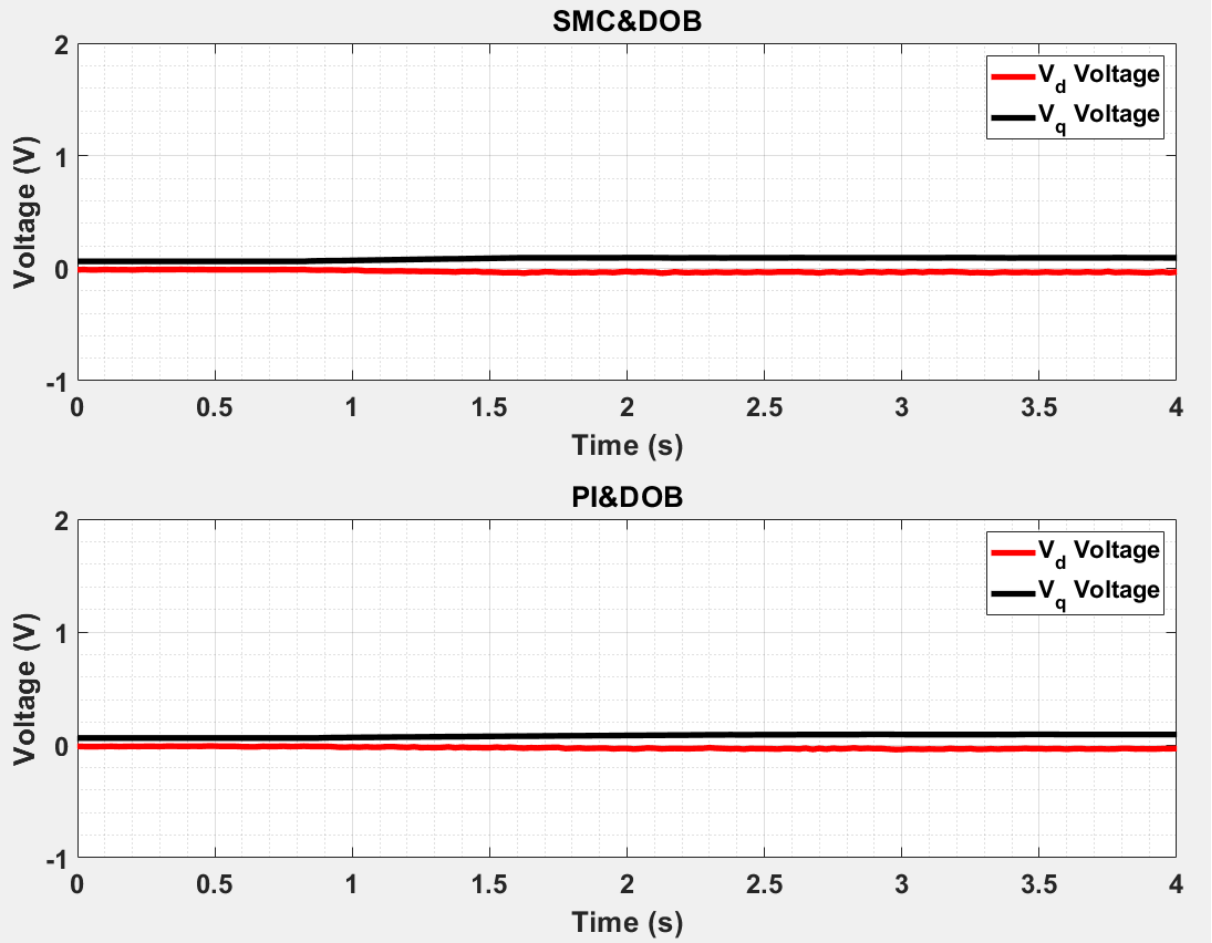

Figure 4-5: Load application experiment, voltage response comparison

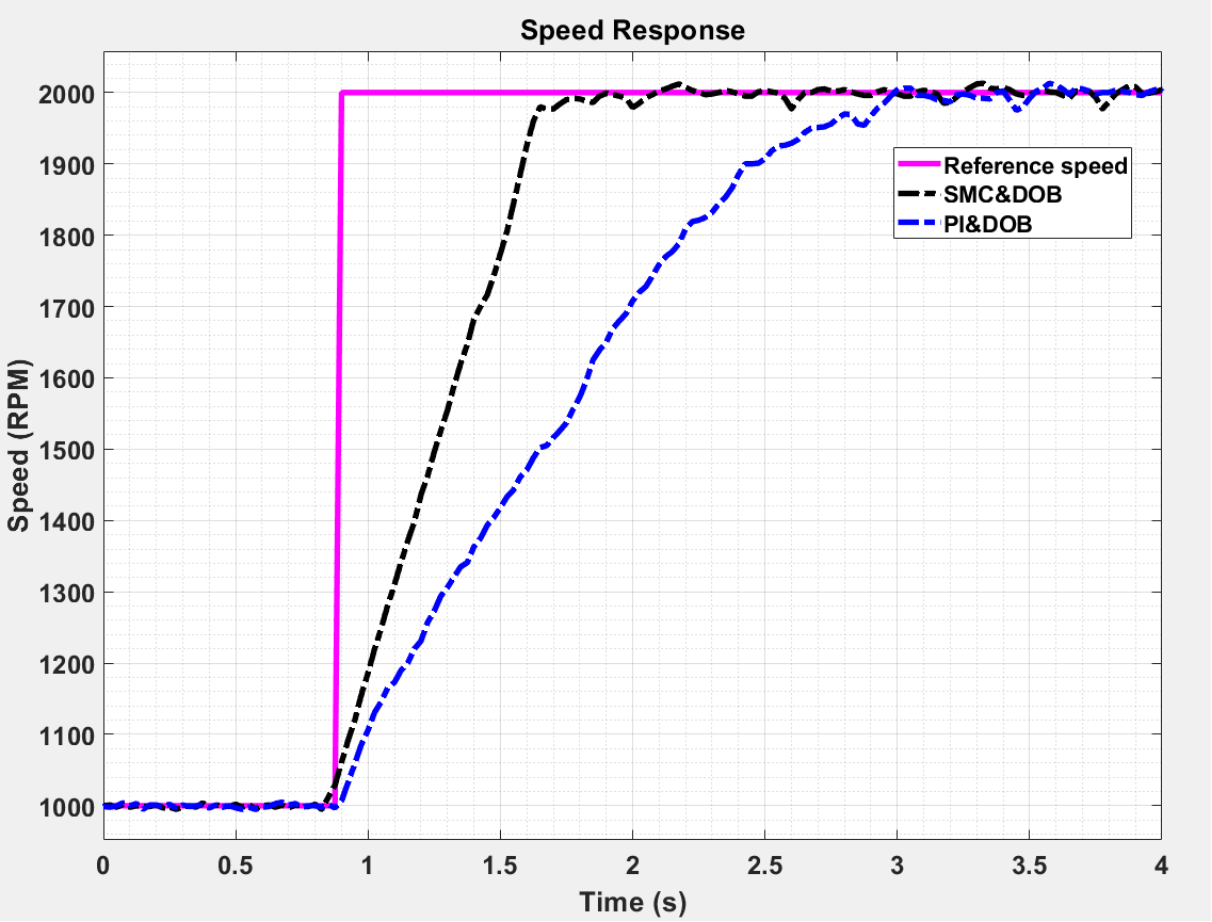

Figure 4-6: Speed step experiment, speed response comparison

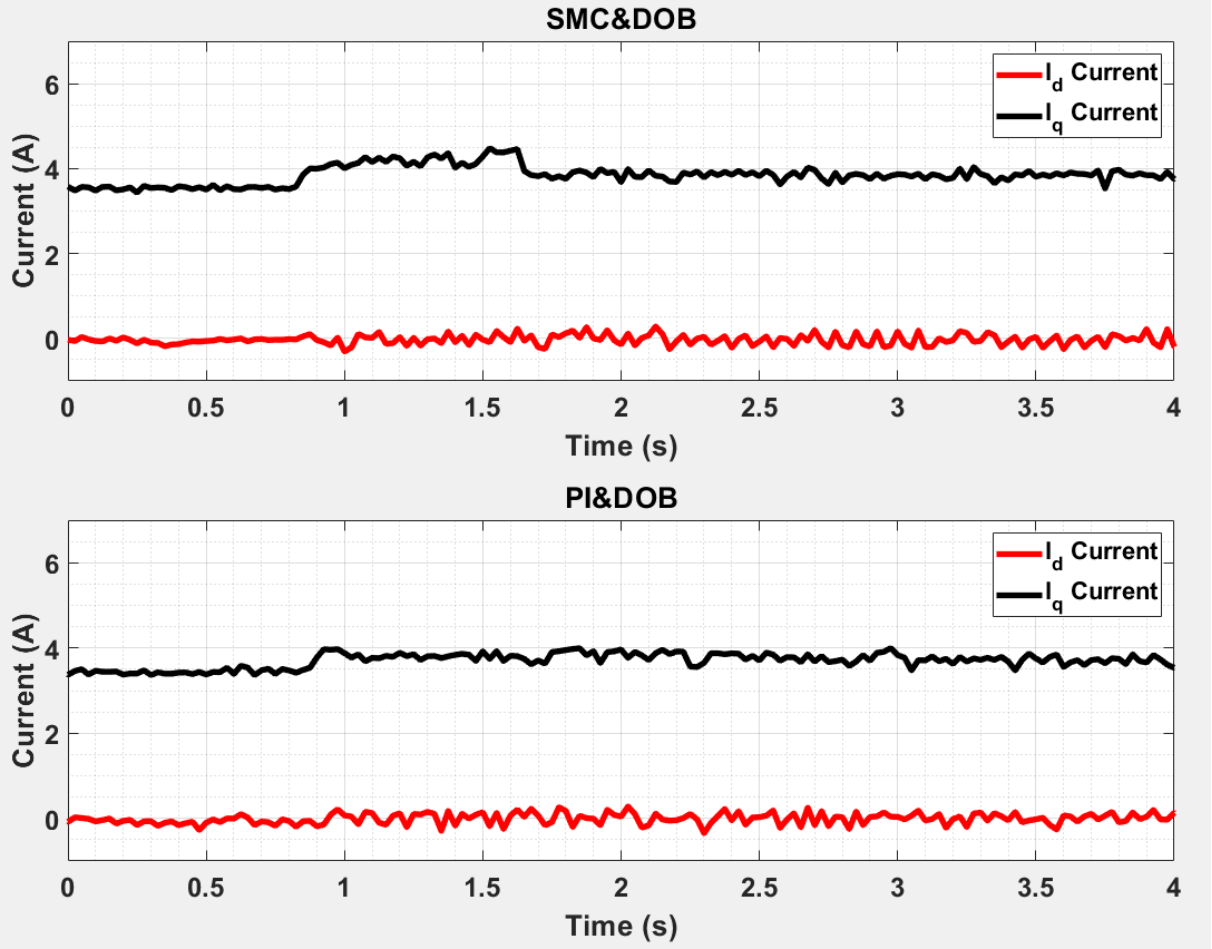

Figure 4-7: Speed step experiment, current response comparison

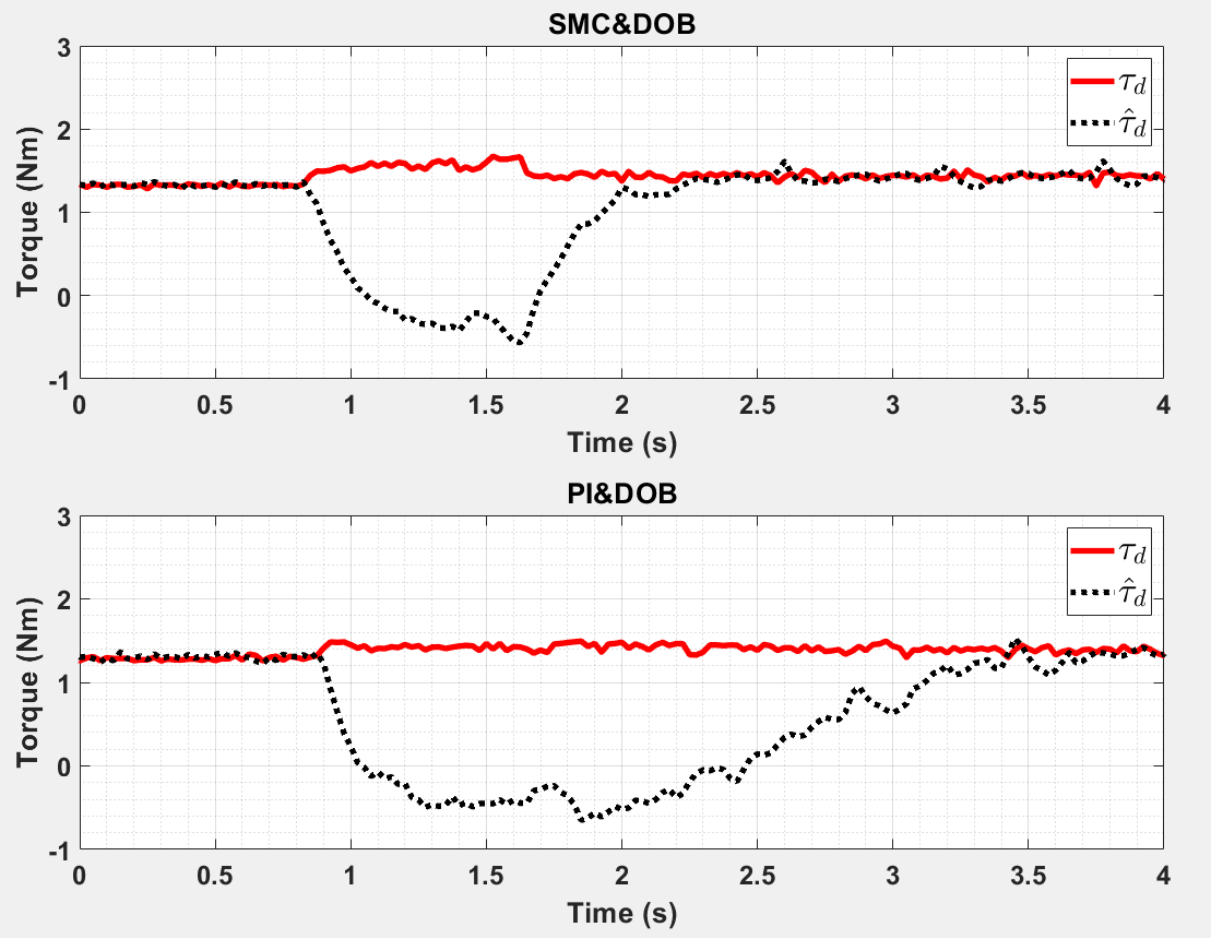

Figure 4-8: Speed step experiment, disturbance estimation comparison

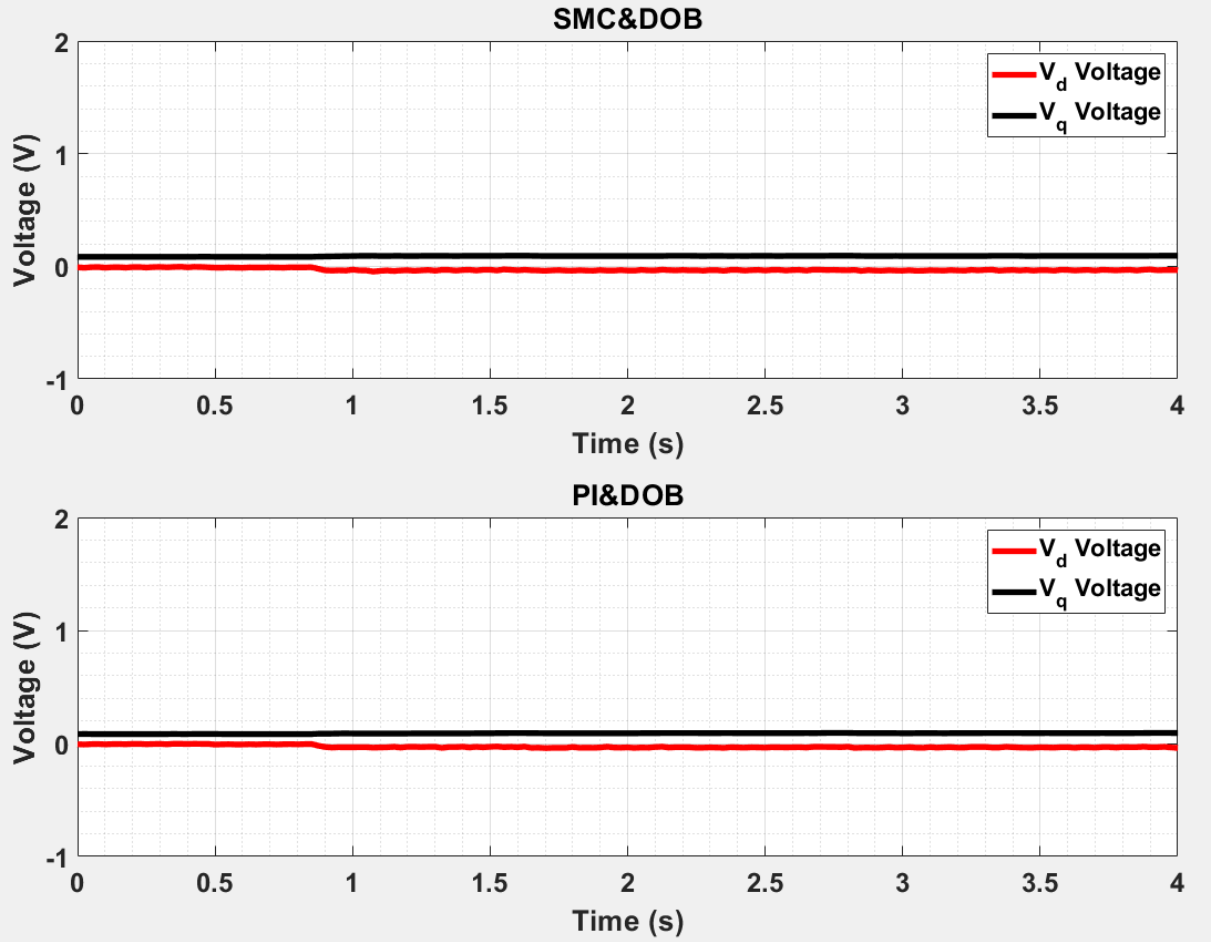

Figure 4-9: Load application experiment, voltage response comparison

Table 4.2: Speed Tracking Performance Comparison (Load Application) [RPM]

Metric	**SMC** J	**PI** J	**SMC** $2J$	**PI** $2J$	**SMC** $3J$	**PI** $3J$
IAE	47.2500	107.4125	45.6250	109.7750	44.2375	117.2750
ITAE	64.4844	99.4269	61.7850	98.7894	59.2669	105.7619
RMSE	37.8476	55.5691	38.6357	57.3021	35.7808	59.7831

From the provided results, it can be clearly seen that proposed SMC controller outperforms PI controller in both experiments. When the load is applied, SMC

Table 4.3: Disturbance Estimation Performance Comparison (Load Application) [Nm]

Metric	**SMC** J	**PI** J	**SMC** $2J$	**PI** $2J$	**SMC** $3J$	**PI** $3J$
IAE	0.4058	0.7382	0.8339	1.5087	1.8117	2.4764
ITAE	0.6085	0.9449	1.2159	1.8244	2.1753	2.7751
RMSE	0.2211	0.3225	0.4963	0.7740	0.8468	1.4295

Table 4.4: Speed Tracking Performance Comparison (Step Experiment) [RPM]

Metric	**SMC** J	**PI** J	**SMC** $2J$	**PI** $2J$	**SMC** $3J$	**PI** $3J$
IAE	1072.0	1205.5	1105.6	1701.8	1094.6	2163.7
ITAE	621.1	897.0	657.9	1820.9	648.8	2954.0
RMSE	0.4975	0.4869	0.5050	0.5682	0.5011	0.6383

Table 4.5: Disturbance Estimation Performance Comparison (Step Experiment) [Nm]

Metric	**SMC** J	**PI** J	**SMC** $2J$	**PI** $2J$	**SMC** $3J$	**PI** $3J$
IAE	1.7692	3.3851	3.4329	6.5444	5.1946	8.2854
ITAE	2.2882	4.9547	4.4641	12.4693	6.7494	17.2705
RMSE	0.8453	1.1732	1.6418	1.9120	2.4460	2.3391

converges back to the reference speed faster than PI, estimated disturbance is also more accurate in case of SMC. Speed step experiment emphasizes the difference in convergence rate between two controllers and accuracy of disturbance estimation.

Another aspect to test these to controllers on is the ability to maintain the performance level while the motor parameter is altered. For this experiment the nominal inertia Jn is doubled and tripled. The obtained responses comparison is provided in figures below.

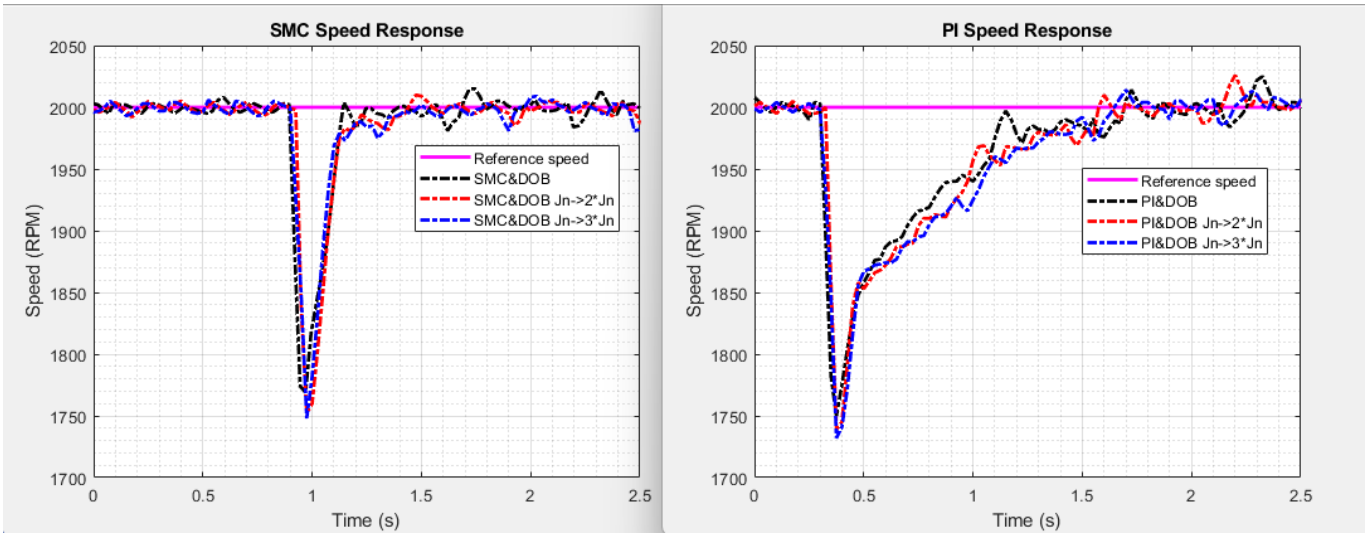

Figure 4-10: Load application experiment, speed response comparison

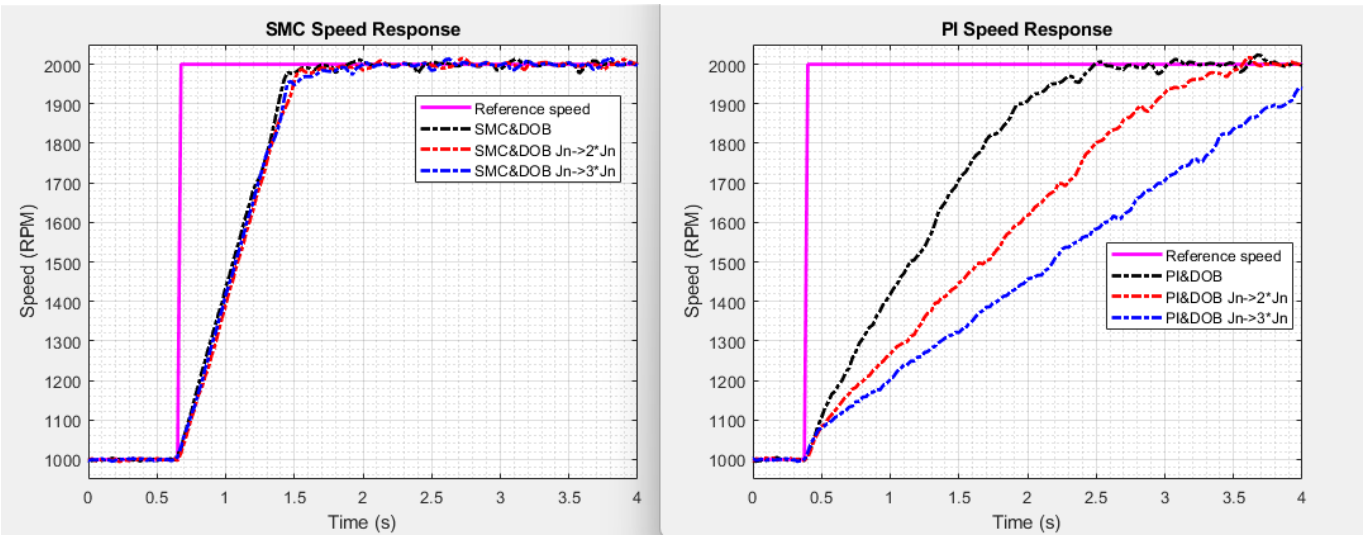

Figure 4-11: Speed step experiment, speed response comparison

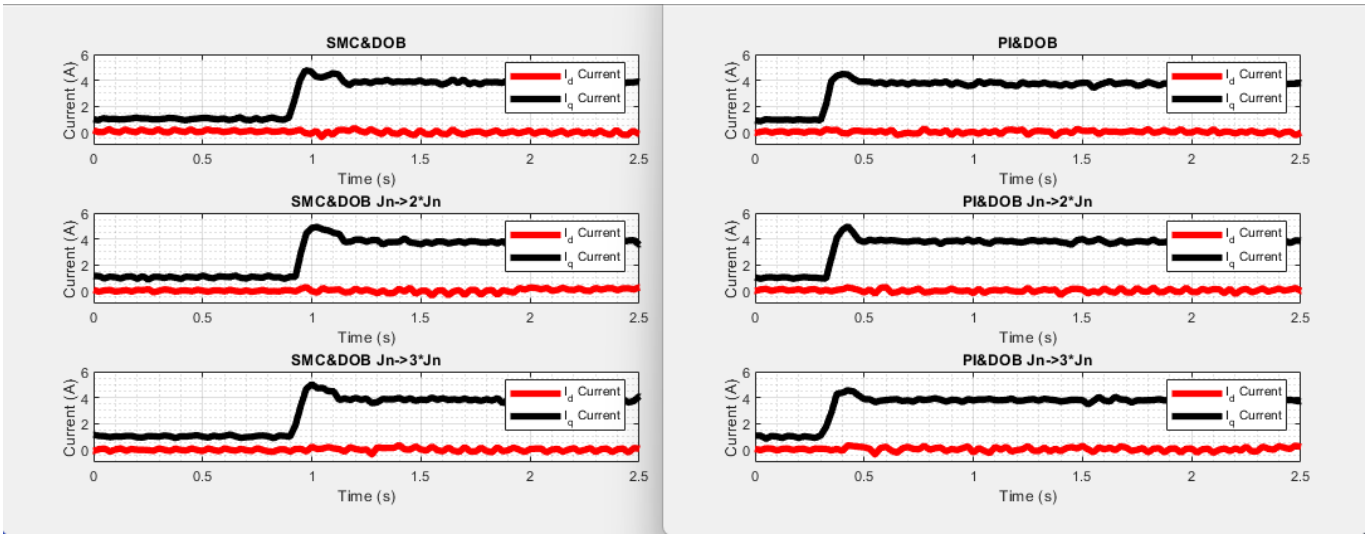

Figure 4-12: Load application experiment, current response comparison

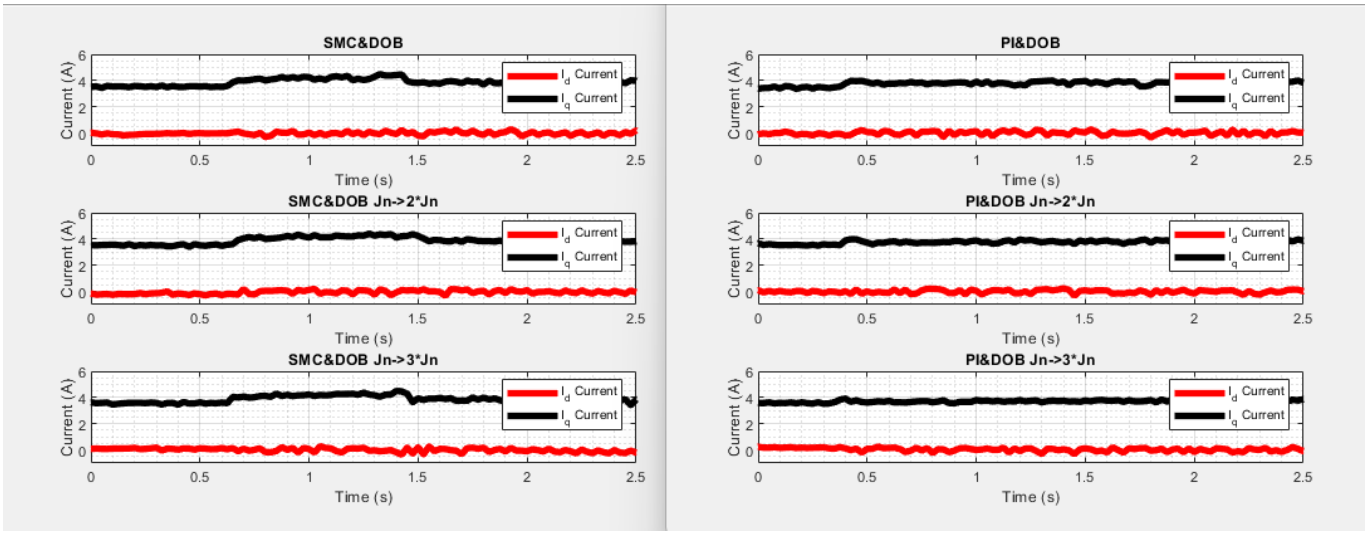

Figure 4-13: Speed step experiment, current response comparison

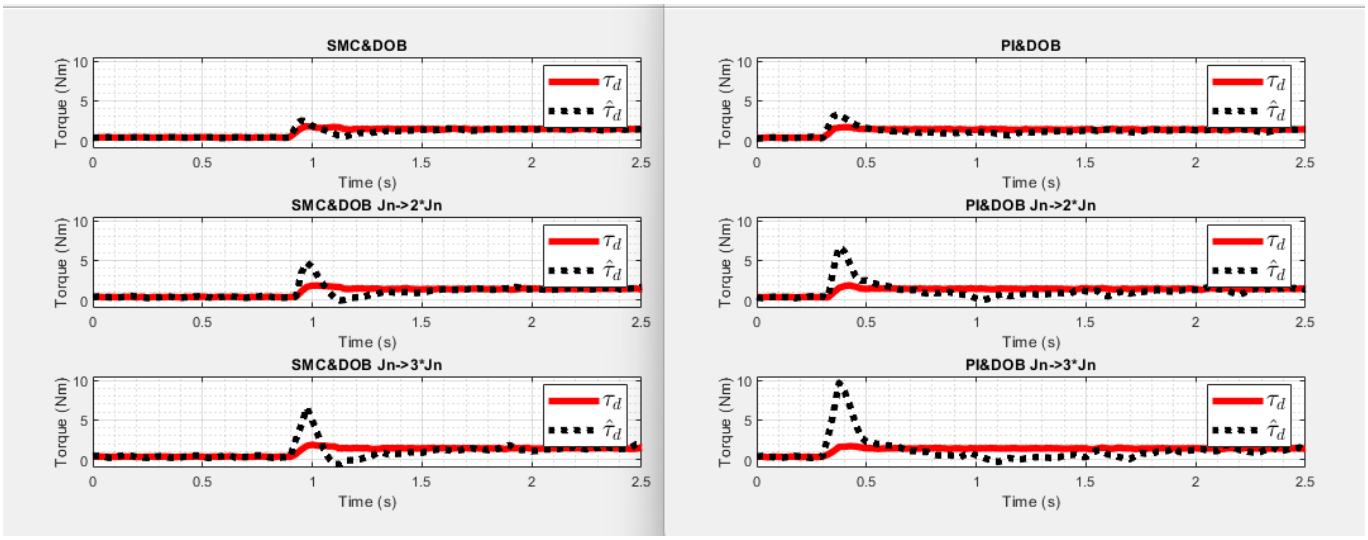

Figure 4-14: Load application experiment, disturbance estimation comparison

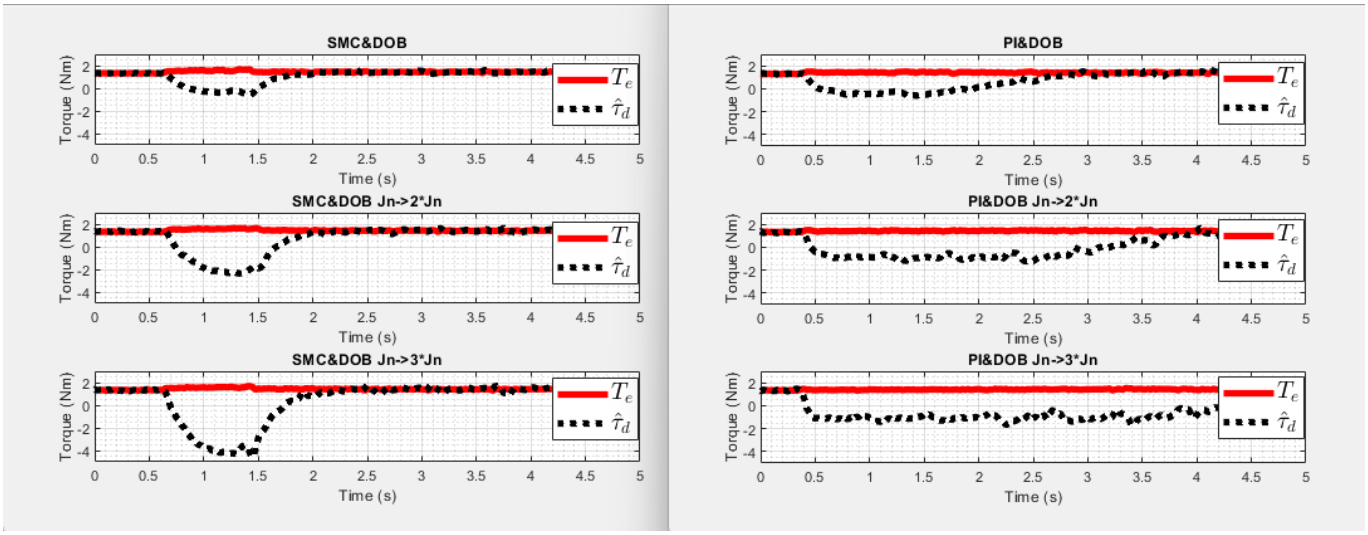

Figure 4-15: Speed step experiment, disturbance estimation comparison

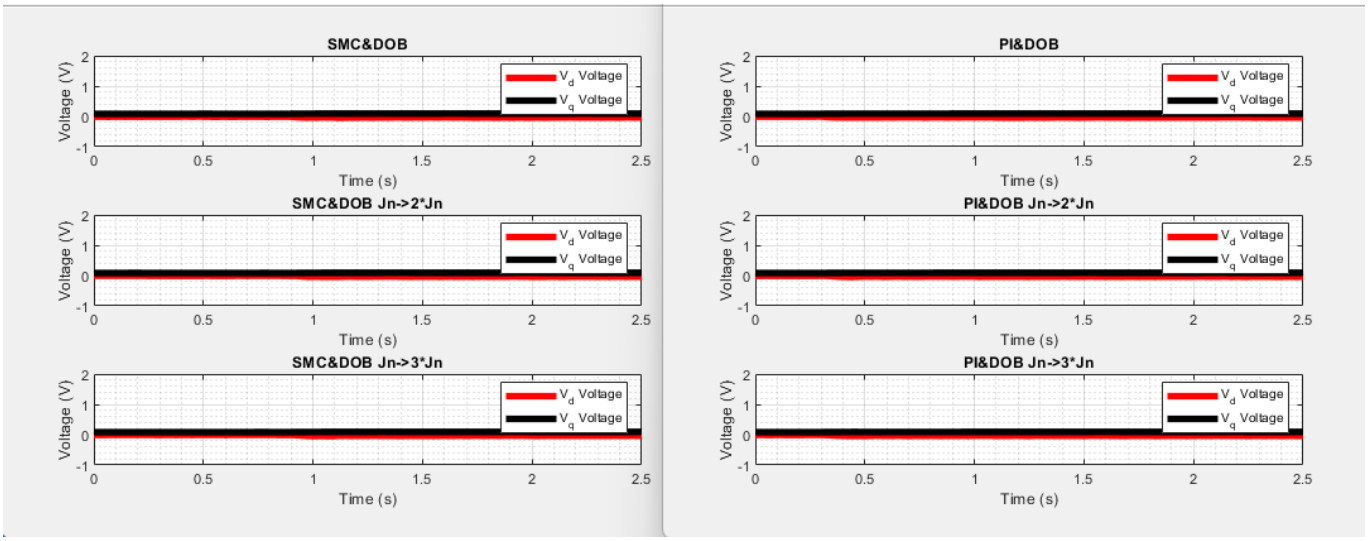

Figure 4-16: Load application experiment, voltage response comparison

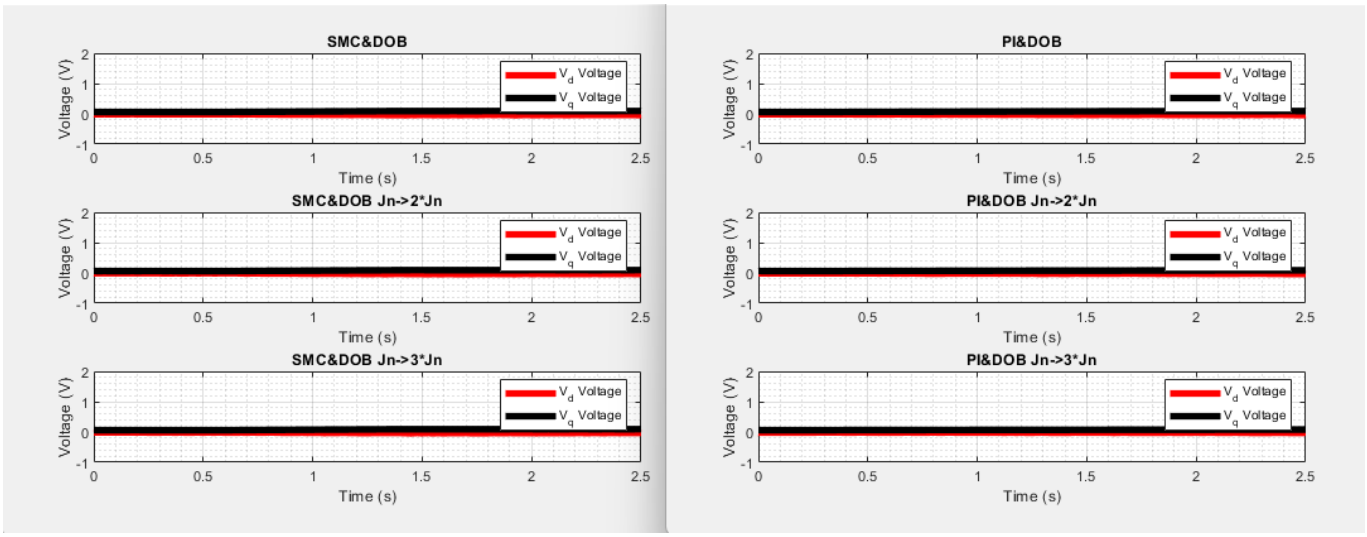

Figure 4-17: Speed step experiment, voltage response comparison

The next simulation is aimed to explicitly show the effect of DOB combined with SMC controller. The speed and current responses of SMC with and without DOB

are compared

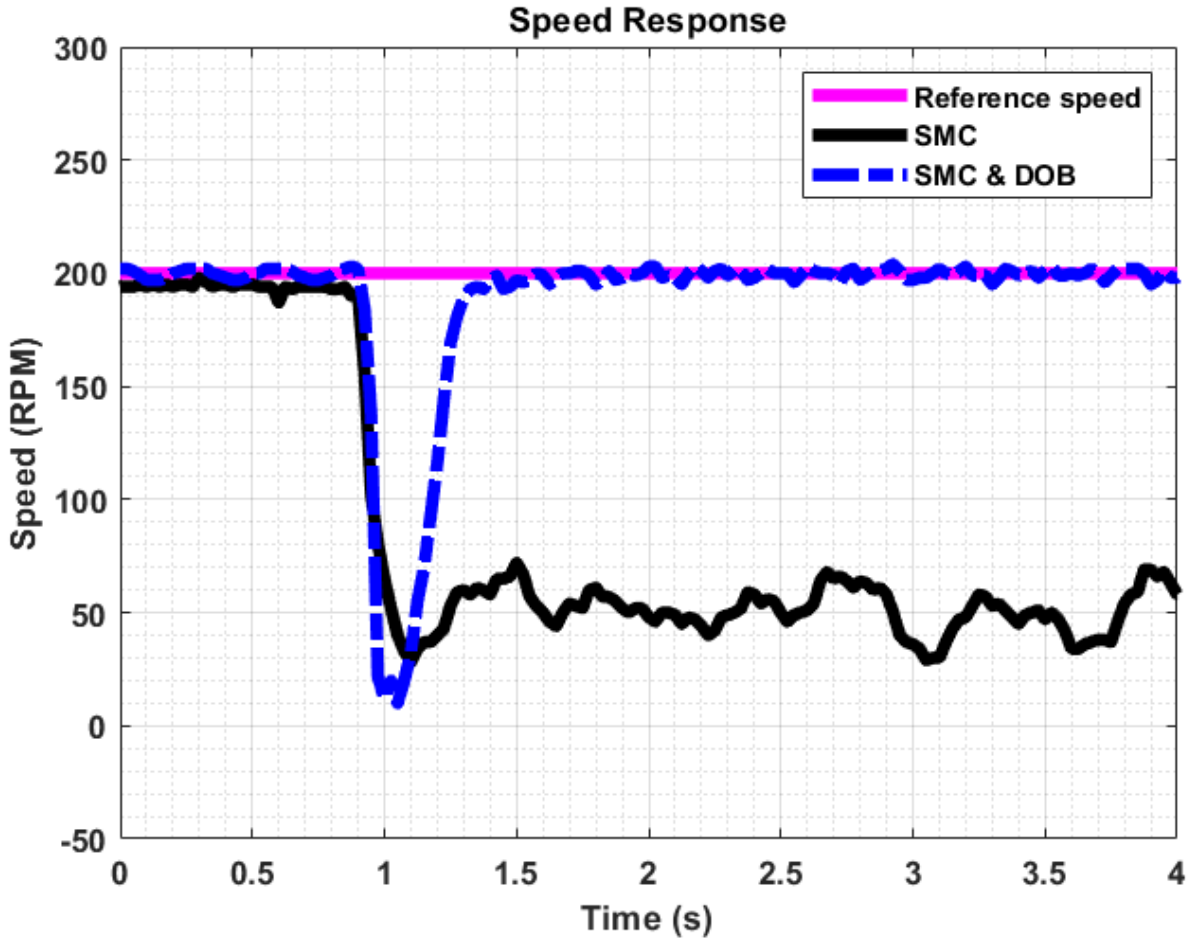

Figure 4-18: SMC vs SMC & DOB, speed response comparison

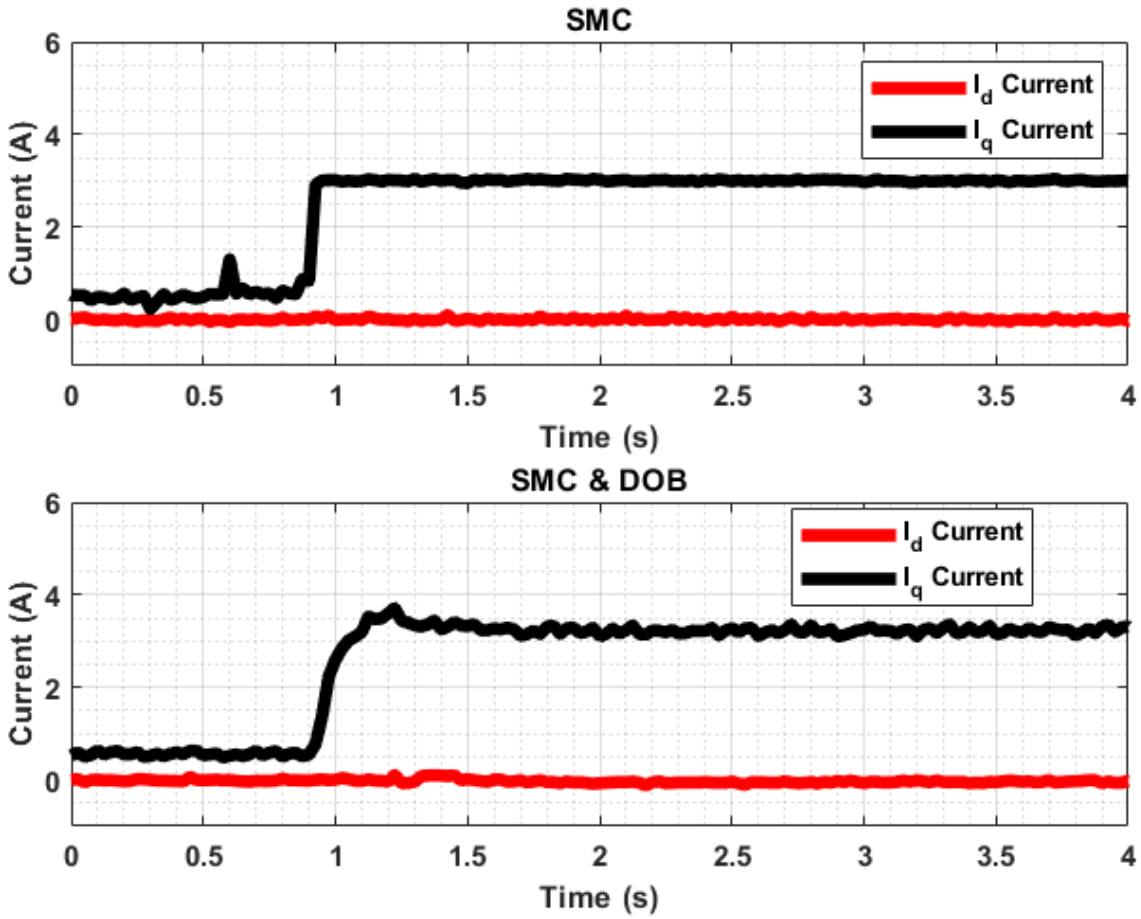

Figure 4-19: SMC vs SMC & DOB, current response comparison

Table 4.6: Speed Tracking Performance Comparison: SMC vs. SMC + DOB [RPM]

Metric	**SMC**	**SMC + DOB**
IAE	426.0	50.0
ITAE	994.0	59.0
RMSE	12.9	4.2

The experiment was conducted under low speed conditions due to the risk of damaging the motor setup while running it with SMC only. From the figures above,

it can be seen that the performance of SMC is poor compared to the response with DOB. In fact, in most of the tries, the setup would not start due to the chattering effect and high spikes in current response. The chosen speed was the maximum speed where the motor managed to work properly and load application would not damage it.

Chapter 5

Conclusion and Future Work

In this thesis, a control strategy based on SMC combined with a DOB was developed and tested for effective speed tracking of PMSMs. The goal was to improve robustness and accuracy, especially in the presence of disturbances and modeling uncertainties that typically affect motor performance.

The DOB helped estimate unknown disturbances in real time, including load torque and friction, allowing the SMC to react appropriately. This combination proved particularly useful in scenarios where the system dynamics were hard to model precisely or where external influences changed over time.

Both simulation and experimental results showed that the proposed controller performed significantly better than the PI controller. It achieved faster transient response, better accuracy, and more reliable behavior under load application and varying inertia conditions. DOB reduced chattering and made the system more stable. Without it, the SMC alone struggled to handle sudden changes or uncertainty effectively.

Overall, the findings show that DOB-aided SMC is a strong combination for prac-

tical PMSM control, offering both robustness and precision. Further improvements can be achieved by tuning the observer and controller parameters adaptively.

Future research can focus on improving the robustness of the proposed control strategy. One potential enhancement is the use of nonlinear or adaptive sliding surfaces to further reduce chattering without losing control performance. Additionally, the disturbance observer can be extended to higher-order or adaptive observer structures to improve estimation accuracy in the presence of measurement noise and model uncertainties. Implementation on embedded platforms such as FPGAs or real-time microcontrollers would allow for deployment in practical industrial systems. The control strategy can also be expanded to include position control or multi-axis PMSM systems. Furthermore, integrating observer-based fault detection mechanisms could improve system reliability and robustness in safety-critical applications.

Bibliography

[1] J. Liu, "Basic sliding mode control principle and design," Elsevier eBooks, pp. 1–29, Jan. 2017, doi: https://doi.org/10.1016/b978-0-12-802575-8.00001-1.

[2] U. Itkis, Control System of Variable Structure, Wiley, New York, 1976.

[3] J.Y. Hung, W. Gao, J.C. Hung, Variable structure control: a survey, IEEE Trans. Ind. Electronics 40 (1) (1993) 222.

[4] C. Edwards, S. Spurgeon, Sliding Mode Control: Theory and Applications, Taylor and Francis, London, 1998.

[5] Sadegh Vaez-Zadeh, Control of Permanent Magnet Synchronous Motors. Oxford University Press, 2018. doi: https://doi.org/10.1093/oso/9780198742968.001.0001.

[6] Bida, V.M., Samokhvalov, D.V. and Al-Mahturi, F.S., 2018, January. PMSM vector control techniques—A survey. In 2018 IEEE Conference of Russian Young Researchers in Electrical and Electronic Engineering (EIConRus) (pp. 577-581). IEEE

[7] Yang, J., Chen, W.H., Li, S., Guo, L. and Yan, Y., 2016. Disturbance/uncertainty estimation and attenuation techniques in PMSM drives—A survey. IEEE Transactions on Industrial Electronics, 64(4), pp.3273-3285.

[8] Zhu, Z.Q., Ruangsinchaiwanich, S. and Howe, D., 2006. Synthesis of cogging torque waveform from analysis of a single stator slot. IEEE transactions on industry applications, 42(3), pp.650-657.

[9] Q. Wang, S. Wang, and C. Chen, "Review of Sensorless Control Techniques for PMSM Drives," IEEJ Transactions on Electrical and Electronic Engineering, vol. 14, no. 3, pp. 596–612, 2019. DOI: 10.1002/tee.22974

[10] L. Dhamo and A. Spahiu, "Simulation Based Analysis of Two Different Control Strategies for PMSM," International Journal of Engineering Trends and Technology (IJETT), vol. 4, no. 4, pp. 596–603, Apr. 2013.

[11] M. S. Merzoug and F. Naceri, "Comparison of Field-Oriented Control and Direct Torque Control for Permanent Magnet Synchronous Motor (PMSM)," World Academy of Science, Engineering and Technology International Journal of Electrical and Computer Engineering, vol. 2, no. 9, pp. 1797–1798, 2008.

[12] S. Hussain and M. A. Bazaz, "Comparative Analysis of Speed Control Strategies for Vector Controlled PMSM Drive," International Conference on Computing, Communication and Automation (ICCCA), pp. 1314–1319, 2016.

[13] C. Cheng, L. Liu, and S. Ding, "Iterative Learning Observer-Based Composite SOSM Control for PMSM Speed Regulation Problem With Mismatched Disturbances," IEEE Transactions on Power Electronics, vol. 39, no. 8, pp. 9470–9482, Aug. 2024. DOI: 10.1109/TPEL.2024.3398775.

[14] L. Samaranayake and S. Longo, "Degradation control for electric vehicle machines using Nonlinear Model Predictive Control," IEEE Transactions on Control Systems Technology, vol. 26, no. 1, pp. 89–101, Jan. 2018. doi:10.1109/tcst.2016.2646322

[15] Z.-X. Fan, S. Li, and R. Liu, "ADP-based optimal control for systems with mismatched disturbances: A PMSM application," IEEE Transactions on Circuits and Systems II: Express Briefs, vol. 70, no. 6, pp. 2057–2061, Jun. 2023. doi:10.1109/tcsii.2022.3233356

[16] J. Li, L. Zhang, L. Luo, and S. Li, "Extended state observer based current-Constrained Controller for a PMSM system in presence of disturbances: Design, analysis and experiments," Control Engineering Practice, vol. 132, p. 105412, Mar. 2023. doi:10.1016/j.conengprac.2022.105412

[17] W. Gao and Z.-P. Jiang, "Adaptive dynamic programming and adaptive optimal output regulation of Linear Systems," IEEE Transactions on Automatic Control, vol. 61, no. 12, pp. 4164–4169, Dec. 2016. doi:10.1109/tac.2016.2548662

[18] Z.-X. Fan, S. Li, and J. Su, "Adaptive Dynamic Programming for PMSM control under safety, robustness, and optimality constraints," IEEE Transactions on Systems, Man, and Cybernetics: Systems, vol. 55, no. 4, pp. 2724–2733, Apr. 2025. doi:10.1109/tsmc.2024.3510544

[19] Shihua Li, Kai Zong, and Huixian Liu, "A composite speed controller based on a second-order model of Permanent Magnet Synchronous Motor System," Transactions of the Institute of Measurement and Control, vol. 33, no. 5, pp. 522–541, Aug. 2010. doi:10.1177/0142331210371814

[20] S. Ding, K. Mei, and S. Li, "A new second-order sliding mode and its application to nonlinear constrained systems," IEEE Transactions on Automatic Control, vol. 64, no. 6, pp. 2545–2552, Jun. 2019. doi:10.1109/tac.2018.2867163

[21] Q. Hou and S. Ding, "GPIO based super-twisting sliding mode control for PMSM," IEEE Transactions on Circuits and Systems II: Express Briefs, vol. 68, no. 2, pp. 747–751, Feb. 2021. doi:10.1109/tcsii.2020.3008188

[22] Y. Shtessel, C. Edwards, L. Fridman, and A. Levine, *Sliding Mode Control and Observation*. Springer New York, 2014.

[23] N. Derbel and R. Chebbah, *Applications of Sliding Mode Control*. Singapore: Springer, 2017.

[24] W. Perruquetti and J.-P. Barbot, *Sliding Mode Control in Electro-Mechanical Systems*, 2nd ed., ser. Automation and Control Engineering. Boca Raton, FL: CRC Press, 2009.

[25] J. Ovalle and L. Fridman, "Sliding mode control for systems with zero-crossing control gain under matched and mismatched disturbances," *Automatica*, vol. 156, p. 111261, 2023.

[26] V. M. Bida, D. V. Samokhvalov, and F. S. Al-Mahturi, "PMSM vector control techniques—A survey," in *Proc. IEEE Conf. Russian Young Researchers in Electrical and Electronic Engineering (EIConRus)*, 2018, pp. 577–581.

[27] D. W. Novotny and T. A. Lipo, *Vector Control and Dynamics of AC Drives*, vol. 41. Oxford University Press, 1996.

[28] D. Casadei, F. Profumo, G. Serra, and A. Tani, "FOC and DTC: Two viable schemes for induction motors torque control," *IEEE Trans. Power Electronics*, vol. 17, no. 5, pp. 779–787, 2002.

[29] F. Amin, E. Sulaiman, and H. A. Soomro, "Field oriented control principles for synchronous motor," *Int. J. Mech. Eng. Robot. Res.*, vol. 8, no. 2, pp. 284–288, 2019.

[30] C. J. O'Rourke, M. M. Qasim, M. R. Overlin, and J. L. Kirtley, "A geometric interpretation of reference frames and transformations: dq0, Clarke, and Park," *IEEE Trans. Energy Convers.*, vol. 34, no. 4, pp. 2070–2083, 2019.

[31] E. Sariyildiz and K. Ohnishi, "A guide to design disturbance observer," *Journal of Dynamic Systems, Measurement, and Control*, vol. 136, no. 2, pp. 021011-1–021011-15, 2014.

[32] A. Shimada, *Disturbance Observer for Advanced Motion Control with MATLAB/Simulink*. IEEE Press and John Wiley & Sons, 2023.

[33] F. M. Zaihidee, S. Mekhilef, and M. Mubin, "Robust speed control of PMSM using sliding mode control (SMC)—A review," *Energies*, vol. 12, no. 9, pp. 1–23, 2019, doi: 10.3390/en12091669.

[34] Y. Zhao and L. Dong, "Robust current and speed control of a permanent magnet synchronous motor using SMC and ADRC," *Control Theory and Technology*, vol. 17, no. 2, pp. 190–199, 2019, doi: 10.1007/s11768-019-8084-y.

[35] H. N. Tran and J. W. Jeon, "Robust speed controller using dual adaptive sliding mode control (DA-SMC) method for PMSM drives," *IEEE Access*, vol. 11, pp. 63261–63273, 2023, doi: 10.1109/ACCESS.2023.3288124.

[36] S. Kumari and A. T. Mathew, "Speed control of permanent magnet synchronous motor drive system using PI, PID, SMC and SMC plus PID controller," in *Proc. IEEE Int. Conf. Power Electron., Drives Energy Syst. (PEDES)*, Chennai, India, Dec. 2018, pp. 1–6, doi: 10.1109/PEDES.2018.8707610.